Investigations with ultracold neutrons

V. K. Ignatovich and V. I. Luschikov

Joint Institute for Nuclear Research, Dubna

Fiz. Elem. Chastits At. Yadra **15**, 330–378 (March–April 1984)

Experimental and theoretical studies in the physics of ultracold neutrons are reviewed. Experimental methods and the interaction of ultracold neutrons with matter and fields are discussed. Possible applications of ultracold neutrons are considered.

INTRODUCTION

The aim of the present review is, briefly and from the historical point of view, to present the main achievements in the physics of ultracold neutrons in both experiment and theory, and also to give an idea of the possible applications of ultracold neutrons as a tool for investigation. The review is intended for a wide audience of physicists, many of whom will have heard about the unusual properties of ultracold neutrons and have ideas about the practical use of these very slow neutrons. We hope that the review will enable them to gauge better the actual possibilities.

Experiments with ultracold neutrons first came to be considered mainly in connection with the necessity of raising the sensitivity of experiments looking for an electric dipole moment of the neutron, and the first suggestion in this direction is due to Shapiro.[1] Now, 14 years later, it can be said that the hopes placed in ultracold neutrons have been justified. At the Leningrad Institute of Nuclear Physics (Gatchina) a group under the direction of V. M. Lobashev has succeeded in reducing the upper limit on the electric dipole moment of the neutron by almost an order of magnitude compared with the limit achieved with faster neutrons.[2] And this is still not yet the limit of the possibilities.

Neutrons are said to be ultracold if they have energy $\lesssim 10^{-7}$ eV. Their characteristic feature is the capacity to be reflected by a number of substances for all angles of incidence. They can be kept in hermetically sealed containers. This property appears paradoxical if one remembers that the very discovery of the neutron was due to its capacity to penetrate readily through fairly thick layers of matter. Nevertheless, it has long been known that thermal neutrons ($E \sim 10^{-2}$ eV) can be completely reflected by matter when their glancing angle with respect to the surface is in the range of a few minutes, this range increasing with decreasing energy E. Hence, extrapolating to ultralow energies, we find that when $E < E_{\text{lim}} \sim 10^{-7}$ eV (E_{lim} is a critical energy characteristic of the given material) the range of angles of total reflection reaches $\pi/2$, i.e., reflection occurs at all angles of incidence.

The phenomenon of total reflection is well known in optics. But whereas in optics light undergoes total internal reflection, i.e., reflection on encountering an interface with vacuum from within matter, neutrons in the majority of cases have the property of total external reflection. This is explained by the fact that matter for neutrons represents a potential barrier of height u_0, and if the energy is $E < E_{\text{lim}} = u_0$, then the reflection is total at all angles of incidence (it will be shown below that $u_0 = 4\pi N_0 b\hbar^2/2m$, where N_0 is the number of atoms per unit volume of the material, b is the amplitude for scattering of a neutron by a nucleus, and m is the neutron mass). In principle, photons can also undergo total external reflection at all angles of incidence, for example, from metals ("metallic reflection"), but for this the square of the refractive index must be negative. Now this is the characteristic feature of ultracold neutrons in a first approximation. More precisely, for neutrons and electromagnetic waves it is necessary to take into account the fact that the refractive index is complex. The corresponding analysis for ultracold neutrons was made by Frank.[3,4]

The possibility of storing ultracold neutrons was first pointed out by Zel'dovich.[5] Later, Drabkin and Zhitnikov[6] considered the possibility of obtaining ultracold neutrons by means of magnetic fields variable in space and time. Vladimirskiĭ[7] showed that neutrons could also be kept in magnetic bottles. He estimated the yield of ultracold neutrons from converters, noted the promise of liquid hydrogen in this respect, and estimated the possibilities of transporting ultracold neutrons in magnetic and vertical channels. He also introduced the expression "ultracold neutrons." Gurevich and Nemirovskiĭ[8] considered metallic reflection of neutrons. In their monograph,[9] Gurevich and Tarasov devoted an entire chapter to ultracold neutrons, which drew the attention of the scientific community to them. Abroad, Foldy[10] took an interest in ultracold neutrons, and suggested that they could be kept in a container with walls covered with superfluid ^{4}He.

However, this was all theory, and, because of their extremely low intensity, ultracold neutrons appeared to be exotic and far from practice. It was only in 1968 that Shapiro and collaborators in Dubna[11] and Steyerl in Munich[12] began real experiments.

1. OBTAINING ULTRACOLD NEUTRONS

The reason why experiments with ultracold neutrons (UCN) began almost 40 years after the discovery of the neutron is their low flux intensity. The flux density of thermal neutrons from a typical research reactor is $\Phi_{\text{th}} = 10^{13}$ cm^{-2}·sec^{-1}, but the flux density of ultracold neutrons is of order 10 cm^{-2}·sec^{-1}. At such an intensity, it would appear that no experiments are possible, but the interest in ultracold neutrons was so great that experimentalists made long and tortuous experiments at fluxes that were actually much lower, when they could achieve acceptable background conditions. For example, in the first experiment the UCN flux density was about 10^{-3} cm^{-2}·sec^{-1}.

Let us estimate the fraction of the total density of an isotropic flux that corresponds to the UCN energy range (0–

 0090-4759/84/020149-23$04.40

E_{lim}) in an ideal Maxwellian spectrum[1]:

$$\Phi_{\text{UCN}} = \Phi_{\text{th}} \int\limits_{k<k_{\text{lim}}} (k_\perp\, d^3k/2\pi T_n^2) \exp(-k^2/T_n)$$
$$\approx (\Phi_{\text{th}}/8)\,(E_{\text{lim}}/T_n)^2\ . \qquad (1)$$

The exponential in the integrand of (1) can be taken equal to unity, since k_{lim}^2 is usually much lower than the neutron temperature T_n. For $T_n = 0.025$ eV (300 °K) and $E_{\text{lim}} = 1.7\times10^{-7}$ eV (the critical energy of copper) $\Phi_{\text{UCN}} = 5\times10^{-12}\Phi_{\text{th}}$, i.e., for $\Phi_{\text{th}} = 10^{-13}$ cm^{-2}·sec^{-1} the UCN flux density is 50 cm^{-2}·sec^{-1}. At such a density, the counting rate of a detector with a window of area 60 cm^2 and efficiency 1 must be $J_{\text{d}} = 3000$ sec^{-1}, and the density of neutrons accumulated in a trap is $n = 16\Phi_{\text{UCN}}/3v_{\text{lim}} = 0.45$ cm^{-3} ($v_{\text{lim}} = \sqrt{2mE_{\text{lim}}} \approx 6$ m/sec). In real experiments, both the detector counting rate and the density of the accumulated neutrons are frequently much less. This occurs mainly because the extracted neturons must be transported far from the reactor to eliminate the strong background of thermal neutrons. The transporting is done in large part by means of long pipes bent in the horizontal plane (neutron guides), within which a vacuum of 10^{-1} Pa (10^{-3} mm Hg) is maintained. The fast neutrons, propagating rectilinearly, pass freely through the walls of the neutron guide, whereas the ultracold neutrons remain within it, being totally reflected by its walls. However, they are partly lost in passage, first because of the loss in the walls and, second, because of diffuse scattering by elements of roughness. The diffuse scattering has the consequence that there is a certain probability for the neutrons to return to the reactor without reaching the detector.[13]

Let us consider methods of obtaining ultracold neutrons. The most common method is to place an additional moderator (converter) within a neutron guide near the reactor. In inelastic collision with nuclei of the converter, thermal neutrons can be decelerated to the UCN energy. In principle, ultracold neutrons are present in the spectrum of the thermal neutrons that leave the surface of the main moderator of the reactor, but in passing to the evacuated neutron guide they are either reflected or absorbed in construction materials. Therefore, it is necessary to regenerate them within the neutron guides. To be specific, we have in mind here horizontal channels. The special features of vertical and inclined channels will be considered below.

The ultracold neutrons produced in the converter may be reheated or absorbed by nuclei. Their loss cross section $\sigma_1 = \sigma_{\text{a}} + \sigma_{\text{ie}}$ (σ_{a} and σ_{ie} are the cross sections for absorption and inelastic scattering, respectively) is large, since it is inversely proportional to the neutron velocity v, while their range $l = 1/N_0\sigma_1 \approx 1$ mm is short. Therefore, the only ultracold neutrons that leave the converter are the ones that were produced in the surface region of thickness l. Obviously, there is no point in making the converter thicker. True, thicker converters can lower the temperature T_n of the neutron spectrum, and in accordance with (1) this increases the UCN yield. However, in practice such thermalization can be achieved only by means of liquid hydrogen.

We now estimate the UCN flux density that can be achieved by means of a converter.[14,15] We denote by $\sigma'_{\text{ie}}(T_c, k_i\to k_f) = d\sigma_{\text{ie}}(T_c, k_i\to k_f)/dk_f$ the differential cross section for inelastic scattering by nuclei of the converter, which has temperature T_c, when the initial neutron energy is $E_i = k_i^2$ and the final $E_f = k_f^2$; $\Phi'(k) = d\Phi(\mathbf{k})/d\mathbf{k}$ is the isotropic spectral flux density of the neutrons with energy $E = k^2$; $\Phi'_\perp(k) = \Phi'(k)k_\perp/k$ is the spectral density of the flux through an element of a given surface (here, $d\mathbf{k} = d^3k = k^2 dk d\Omega; d\Omega = d\varphi d(\cos\theta)$, and $k_\perp = k\cos\theta$ is the component of the wave vector $\mathbf{k}$ normal to the surface).

It is obvious that for ultracold neutrons with energy $E_0 = k_0^2$

$$\Phi'_{\perp\text{UCN}}(k_0) = \Phi_{\text{th}}(k_{0\perp}/k_0)\,\overline{\sigma'_-(T_c,\ k\to k_0)\,N_0 l\,(k_0)}$$
$$= \Phi_{\text{th}}(k_{0\perp}/k_0)\,\overline{\sigma'_-(T_c,\ k\to k_0)}/[\sigma_a(k_0) + \sigma_+(T_c,\ k_0)], \qquad (2)$$

where

$$\overline{\sigma'_-(T_c,\ k\to k_0)} = \int \sigma'_{ie}(T_c,\ k\to k_0)\,\theta(k^2 > k_0^2)$$
$$\times\, e^{-k^2/Tn}\, k\, d\mathbf{k}/2\pi T_n^2 \qquad (3)$$

is the differential cross section for cooling, averaged over the spectrum of thermal neutrons. The inetgral contains the θ function, which is equal to unity when the inequality indicated in its argument is satisfied and zero otherwise. The heating cross section $\sigma_+(T_c, k_0)$, which occurs in (2), is

$$\sigma_+(T_c,\ k_0) = \int \sigma'_{ie}(T_c,\ k_0\to k)\,\theta(k^2 > k_0^2)\,d\mathbf{k} \approx \sigma_{ie}(T_c,\ k_0). \qquad (4)$$

The expression (2) can be simplified by using the principle of detailed balance, according to which the interaction with matter must not change the Maxwellian distribution of the neutrons when $T_n = T_c$. This principle can be expressed as equality of the rates of transition from the state with wave vector $\mathbf{k}$ to the state with wave vector $\mathbf{k}_0$ and vice versa:

$$k\, d\mathbf{k}\sigma'_{ie}(T_c,\ k\to k_0)\, e^{-k^2/T_c}\, d\mathbf{k}_0 = k_0\, d\mathbf{k}_0\sigma'_{ie}(T_c,\ k_0\to k)$$
$$\times\, e^{-k_0^2/T_c}\, d\mathbf{k}. \qquad (5)$$

It follows that we can write $\sigma'_{\text{ie}}(T_c), k\to k_0) = F(T_c, k, k_0)(1/k)\exp(-k_0^2/T_c)$, where $F(T_c, k, k_0)$ is a function symmetric with respect to interchange of k and k_0. In addition, $\sigma'_{\text{ie}}(T_c, (k\to k_0) = k_0/k)\exp[(k^2 - k_0^2)/T_c]\,\sigma'_{\text{ie}}(T_c, k_0\to k)$. Substituting this relation in (3), we obtain

$$\overline{\sigma'_-(T_c,\ k\to k_0)} = k_0 \int \sigma'_{ie}(T_c,\ k_0\to k)\,\theta(k^2 > k_0^2)$$
$$\times \exp[-(k_0^2 - k^2)/T_c - k^2/T_n]\, d\mathbf{k}/2\pi T_n^2. \qquad (6)$$

In particular, for $T_c = T_n$ we have $\overline{\sigma'_-(T_c, k\to k_0)} \sim \sigma_+(T_c, k_0)$ since $k_0^2 \ll T_c$. Accordingly,

[1]In all that follows, except when specially stated, all quantities in expressions having the dimensions of energy will be divided by $\hbar^2/2m$, where m is the neutron mass. For example, if square brackets indicate quantities in their natural dimensions, then $E = (2m/\hbar^2)[E] = k^2 = [k^2]$, where k is the wave vector (in particular, $E_{\text{lim}} = k_{\text{lim}}^2$); the temperature is $T = (2m/\hbar^2)k_{\text{B}}[T]$, where k_{B} is Boltzmann's constant; $\omega = (2m/\hbar^2)\hbar[\omega] = (2m/\hbar)[\omega]$ is expressed in cm^{-2}, and accordingly the time $t = (\hbar/2m)[t]$ is expressed in cm^2. Of course, whenever there is a ratio of two energies, any convenient dimension can be used.

$$\Phi_{\text{UCN}} = \int_0^{k_{11\text{m}}} \Phi'(k_0)\, d\mathbf{k}_0$$

$$= (\Phi_{\text{th}}/8)\,(E_{11\text{m}}/T_n)^2\,\sigma_+(T_c,\ k_{11\text{m}})/[\sigma_a(k_{11\text{m}}) + \sigma_+(T_c,\ k_{11\text{m}})]. \quad (7)$$

It is obvious that k_{lim} in the arguments of σ_a and σ_+ can be replaced by any other wave vector, since these cross sections are proportional to $1/k$ and their ratio does not depend on k.

For $\sigma_a = 0$, Eq. (1) follows from (7). When $T_c \neq T_n$, we must replace $\sigma_+(T_c, k_{\text{lim}})$ in the numerator of the expression (7) by the cross section

$$\tilde{\sigma}_+(T_c,\ T_n,\ k_{11\text{m}}) = \int \sigma'_+(T_c,\ k_{11\text{m}} \to k) \times \exp[-k^2(1/T_n - 1/T_c)]\, d\mathbf{k}. \quad (8)$$

For given T_n, the UCN yield increases with decreasing T_c in the majority of cases (if σ_a is not large). This fact can be used, since the temperature of the converter can be varied independently of the temperature of the main moderator.

The converter can be either a solid, a liquid, or a gas, but in the last two cases it must be placed in a container sufficiently transparent for the ultracold neutrons. A solid must be radiation-stable and have a low critical energy $E_{\text{lim,c}}$. The existence of $E_{\text{lim,c}}$ leads to three effects. First, neutrons produced within the converter acquire an additional kinetic energy equal to $E_{\text{lim,c}}$ when leaving it. Therefore, in the UCN spectrum in the neutron guide there are not neutrons with energy $E < E_{\text{lim,c}}$. (Strictly speaking, there are such neutrons, but their number is very low, since they are produced in a layer of thickness $1/\sqrt{u_c} \ll -l$.) Second, the presence of $E_{\text{lim,c}}$ produces a potential jump at the surface of the converter, which makes it difficult for the produced ultracold neutrons to escape because of reflection at the interface. But the same jump prevents their penetration into the converter and perishing there. The last property of $E_{\text{lim,c}}$ is helpful, and it would be desirable to decrease $E_{\text{lim,c}}$ for the produced neutrons but to increase it for those returning to the converter. In pulsed reactors, this can be done by using mechanical screens, moving the material, or its magnetic and thermal properties.[16] Besides a low $E_{\text{lim,c}}$, the material of the converter must, as follows from (7), have a large ratio $\sigma_{\text{ie}}/\sigma_a$. Hydrogen satisfies all these requirements best. The requirement of a low $E_{\text{lim,c}}$ can be lifted if the ultracold neutrons are extracted by means of a vertical channel, since the ascending neutrons are decelerated by the gravitational field (in rising 1 m, a neutron is decelerated by 10^{-7} eV). A vertical channel was used, for example, in Ref. 18.

The simplest converter having a comparatively high UCN generation efficiency is zirconium hydride. The flux density obtained by means of a ZrH_2 plate 1.5-mm thick with $\varnothing = 70$ mm was 55 $\text{cm}^{-2}\cdot\text{sec}^{-1}$ for $\Phi_{\text{th}} = (2\text{–}4)\times 10^{14}$ $\text{cm}^{-2}\cdot\text{sec}^{-1}$.[17] Also promising is a converter with water frozen onto a substrate at 80 °K.[15] The record UCN flux density (about 1000 $\text{cm}^{-2}\cdot\text{sec}^{-1}$ for $\Phi_{\text{th}} = 6\times 10^{13}$ $\text{cm}^{-2}\cdot\text{sec}^{-1}$) was obtained with a liquid-hydrogen converter at the Leningrad Institute of Nuclear Physics at Gatchina.[18] In the literature,[19] there has also been a discussion of the possibility of using superfluid helium as a converter. In it there is no absorption and incoherent scattering at all. Coherent inelastic scattering takes place on phonons and rotons. The conservation law for energy and momentum has the consequence that the neutron energy can be changed by scattering only discretely by $\Delta E = 2mc^2 = 12$ °K, where c is the velocity of sound in the helium. Thus, we appear to be dealing with a two-level system. In this case, the inelastic-scattering cross section can be represented in accordance with (5) and other general considerations in the form

$$\sigma'_{ie}(T_c,\ k_i \to k_f) = (1/k_i)\exp(-k_f^2/T_c)\, f(k_i,\ k_f) \times [\delta(k_i^2 - k_f^2 - \Delta E)\exp(k_f^2/T_c) + \delta(k_f^2 - k_i^2 - \Delta E)\exp(k_i^2/T_c)], \quad (9)$$

where f is a symmetric function. Hence, using (7) and (8), we obtain

$$\Phi_{\text{UCN}} = (\Phi_{\text{th}}/8)\,(E_{\text{lim}}/T_n)^2 \exp[-\Delta E\,(1/T_n - 1/T_c)]. \quad (10)$$

This quantity can become even larger than $(\Phi_{\text{th}}/8)(E_{\text{lim}}/T_c)^2$ if $T_c^2 \exp(\Delta E/T_c) > T_n^2 \exp(\Delta E/T_n)$. The first experiment[20] confirmed the possibility of using helim as a UCN converter.[2)]

There are other ways of obtaining ultracold neutrons, for example, mechanical deceleration as a result of reflection of more energetic neutrons by moving mirrors.[21] If a neutron with velocity v catches up with a mirror moving with velocity u, then after reflection the normal component of its velocity is reduced by $2(v_\perp - u)$. If diffraction phenomena are not used, single reflection changes the neutron energy little, since $v_{\text{lim}} - u$ cannot be greater than v_{lim} of the mirror. The neutron velocity is reduced appreciably by multiple reflection. This was the principle used in the construction of Steyerl's turbine[22] with curved blades, in which a neutron was repeatedly reflected by a blade, gliding along it and being decelerated as a result of successive reflections from the initial velocity 50 m/sec to 5 m/sec. A different turbine, of Kashukeev,[23] had straight blades, but the neutron slid along the blade from the periphery to the center, being decelerated in the field of the centrifugal potential from an initial velocity of ~70 m/sec.

If one uses the diffraction phenomenon, i.e., the phenomenon of Bragg reflection at thermal energies, deceleration can take place from higher velocities. An experiment of this kind was made at the Argonne Laboratory.[24] The neutrons were reflected from a crystal moving with velocity 200 m/sec and were decelerated from an initial velocity of 400 m/sec.

An intermediate variant is also possible. The critical velocity can be raised by using so-called supermirrors, which are a system of thin films of variable thickness with alternating potentials.[25] In Ref. 26 there is a proposal to make a turbine with blades of supermirrors and critical velocity 15 m/sec.

It is interesting to note that mechanical deceleration of neutrons of a Maxwellian spectrum cannot give more ultracold neutrons than there already are in the spectrum—because of Liouville's theorem—but it may be the preferable

[2)]Recently, a UCN density in liquid helium of about 30 cm^{-3} was obtained.[152]

method if the initial spectrum is nonequilibrium. In addition, one can also avoid using neutron guides, which lead to a strong attenuation of the UCN beam.

2. TRANSPORTING ULTRACOLD NEUTRONS

As we have already pointed out, neutron guides appreciably attenuate the UCN flux. They create a resistance to the flux that is higher, the greater the ratio $\mathscr{L} = L/r$ of the length to the radius and, in addition, depends on the treatment of the internal surface, since this affects the reflection of neutrons by the wall. The transmission $W_{\rm tr}(\mathscr{L})$ of a neutron guide is defined as the ratio $W_{\rm tr}(\mathscr{L}) = J(\mathscr{L})/J(0)$, where $J(\mathscr{L})$ and $J(0)$ are the fluxes at the exit and entrance, respectively. If the walls are well polished, the reflection is almost specular, and the transmission can be estimated if one knows the approximate number of neutron impacts on the wall and the loss in each impact. In the loss one must also include a small fraction of nonspecular reflection, which returns the ultracold neutrons to the converter. (Here, we consider only horizontal neutron guides; in the vertical and inclined case diffuse reflection from the walls can lead to loss of a decelerated neutron through the walls.) The best, not too long neutron guides attenuate the UCN flux linearly (by 30% for $\mathscr{L} = 100$).

If the polishing is not good, the reflection from the walls is mainly nonspecular, and neutron propagation through the neutron guide can be described by the laws of diffusion.[13,27,28] In this case, the transport of ultracold neutrons resembles the flow of a rarefied gas. A difference is that gas molecules are not lost when they collide with the walls and their reflection by the walls is largely diffuse, i.e., the probability of reflection in the direction Ω is proportional to $\cos\theta$, where θ is the angle between Ω and the normal to the surface, and it does not depend on the angle of incidence. The UCN reflection indicatrix $W_{\rm ref}(\Omega_0,\Omega)$, which determines the probability of reflection in the direction Ω if the neutron is incident from the direction Ω_0, can have a more complicated form. However, this form is not entirely arbitrary. The requirement of the principle of detailed balance, the essence of which is that for an isotropic UCN distribution the reflection cannot change the isotropy, leads [by analogy with (5)] to the expression $W_{\rm ref}(\Omega_0,\Omega) = F(\Omega_0,\Omega)\cos\theta$, where $F(\Omega_0,\Omega)$ is an aribitrary but symmetric function of its arguments. As an example, we can give the indicatrix of nonspecular reflection in the presence of elements of roughness.[29] If the elements have rms height $\zeta_0 \ll \lambda_{\rm lim} = 1/\sqrt{u_0}$ and the characteristic dimension along the surface is l (an electron microscope shows that on the electrolytically polished surface of copper $\zeta_0 \leqslant 10$ nm, $l \approx 35$ nm), then the indicatrix of nonspecular reflection has the form

$$W_{ns}(\Omega_0,\ \Omega) = (2/\pi)\,\zeta_0^2 l^2 k k_{0\perp} k_\perp^2 \exp\left[-(\mathbf{k}_{0\parallel} - \mathbf{k}_\parallel)^2 l^2/2\right], \tag{11}$$

where $\mathbf{k}_\parallel$ and $k_\perp$ are the components of the wave vector along the plane and the normal, respectively. If a thermal neutron is incident on the surface at an angle larger than the critical, the reflected neutron may leave the range of angles of total reflection and have a greater probability for entering the material than for being reflected. In this case, the reflection indicatrix is rather the scattering indicatrix and has the form[29]

$$W_{ns}(\Omega_0,\ \Omega) = (1/2\pi)\,\zeta_0^2 l^2 u_0 k k_{0\perp} \exp\left[-(\mathbf{k}_{0\parallel} - \mathbf{k}_\parallel)^2 l^2/2\right]. \tag{12}$$

To calculate the transmission of ultracold neutrons by neutron guides, the Monte Carlo method is most generally used. The reflection indicatrix with allowance for the specularity has in the general case the form

$$W_{\rm ref}(\Omega_0,\ \Omega) = (1 - \psi(\Omega))\,\delta(\Omega - \Omega_0) + W_{ns}(\Omega_0,\ \Omega), \tag{13}$$

where $\psi(\Omega)$ is determined by the normalization condition:

$$\int W_{\rm ref}(\Omega_0,\ \Omega)\,d\Omega = 1. \tag{14}$$

To simplify the calculations, we can take[30]

$$W_{\rm ref}(\Omega_0,\ \Omega) = (1 - gA(\Omega))\,\delta(\Omega - \Omega_0) + cgA(\Omega_0)\,A(\Omega)\cos\theta, \tag{15}$$

where g is the parameter of nonspecularity, and c is a normalization constant. For $A(\Omega) \equiv 1$, the nonspecular part of the reflection is purely diffuse, i.e., it does not depend on the angle of incidence. For $A(\Omega) = \cos\theta$, the reflection is more realistic, since in this case the probability of nonspecular reflection decreases with increasing angle of incidence. In calculations, the indicatrix (11) has been used.[31]

From calculations of straight neutron guides there follows an interesting fact, which has been confirmed by experiments.[32] It is that the angular distribution at the exit from the neutron guide is elongated along the axis if the distribution at the entrance is isotropic. This fact can be readily understood by bearing in mind that the UCN density along the neutron guide decreases monotonically from the entrance opening to the exit. The smaller the axis between the neutron guide and the direction of emergence of a neutron, the closer to the entrance the section of the wall from which it must emerge. The number of neutrons reflected from the surface is proportional to the UCN density at the given point, and therefore it is larger, the closer the corresponding section of the surface to the entrance. There will be an isotropic (in the forward hemisphere) distribution at the exit only in the case of perfectly specular reflection from the walls and an isotropic distribution at the entrance.

In the case of sufficiently strong nonspecular reflection, the transmission of a neutron guide can be calculated in the diffusion approximation. In this approximation, the flux $J(z)$ at a point z along the axis of the neutron guide is determined by the expression $J(z) = -Ddn(z)/dz$, where D is the diffusion coefficient and $n(z)$ is the linear UCN density. In the most general case when $n(z)$ also depends on the time t, we have for $n(z,t)$ the diffusion equation

$$\partial n(z,\ t)/\partial t = -D\,\Delta n(z) - n(z)/\tau. \tag{16}$$

Here, τ is a characteristic time equal to the storage time of ultracold neutrons in a neutron guide closed at both ends. The solution of this equation is determined by the initial and boundary conditions. The boundary conditions contain the entrance flux $J(0)$ and the conditions of reflection at the ends

of the neutron guide. Determining the flux $J(z)$ at $z = \mathscr{L}$ in accordance with the diffusion formula, and dividing it by $J(0)$, we find the transmission $W_{tr}(\mathscr{L})$. In a steady regime, for large $\mathscr{L}$ the transmission is proportional to $\exp(-\mathscr{L}/\mathscr{L}_d)$,[27] where $\mathscr{L}_d$ is the diffusion length: $\mathscr{L}_d = \sqrt{D\tau}$. It is of interest to determine D and τ separately and to compare these quantities with the theoretical values. For example, for the reflection indicatrix (15) with $A(\Omega) \equiv 1$ we have diffusion coefficient $D = (2/3)rv(2-g)/g$, where v is the neutron velocity. Knowing D and the UCN spectrum, we can estimate the parameter of nonspecularity g. Measuring τ, we can determine the loss coefficient for neutron impact on the wall. This will be discussed below. However, measuring the dependence $W_{tr}(\mathscr{L})$ at different $\mathscr{L}$, we determine only the combination $\sqrt{D\tau}$. In Ref. 27, for example, it was found that in a chemically polished copper neutron guide $\sqrt{D\tau} = 100$. One of the ways of separate measurement of D and τ is to fill the neutron guide with ^{4}He gas (it is atomic, is not adsorbed on the surface, and has zero absorption), and to measure $\mathscr{L}_d$ at different pressures p. In the presence of helium, the storage time τ is transformed into τ_p: $1/\tau_p = 1/\tau + p/(p\tau)_{He}$. Here, $(p\tau)_{He}$ is a constant. It can be determined as follows. The flux density of ^{4}He atoms onto a neutron almost at rest is $n_{He}v_{He}$, where n_{He} and v_{He} are, respectively, the density and velocity of the helium atoms. If we denote the cross section for scattering of the neutron by σ_{He}, then the number of collisions with ^{4}He atoms per unit time is $n_{He}v_{He}\sigma_{He}$. Since $n_{He} = p/k_BT$, this number can be written in the form $pv_{He}\sigma_{He}/k_BT$, so that for constant $(p\tau)_{He}$ we obtain the expression $(p\tau)_{He} = k_BT/v_{He}\sigma_{He} = 343$ mm Hg·sec at $T = 300$ °K. Measuring $\mathscr{L}_d$ at different p, we obtain for $1/\mathscr{L}_d^2$ the linear function $1/\mathscr{L}_d^2 = (1/D)(1/\tau + p/(p\tau)_{He})$, from which D and τ can be determined.

In principle, the parameters D and τ can be found by measuring the dependence of J on p for one length of the neutron guide (the so-called helium curve), but the corresponding theoretical curve has a more complicated form, and the fitting procedure is accordingly more complicated. In Ref. 27, a simple method was used, namely, a diaphragm was placed at the exit of the neutron guide, and the flux was measured as a function of the area of the diaphragm opening. As a result of these measurements it was found that time τ was 10 times less than the theoretical time, and the probability of nonspecular reflection was about 10%.

In a well-polished neutron guide, the nonspecularity may be much less. If the nonspecularity is characterized by a parameter $g \ll 1$, the diffusion approximation (16) is invalid. In this case, it can be assumed that with probability $g/2$ the neutron turns back at each collision with the wall, as a result of which the forward flux is attenuated. For not too long neutron guides, for which the approximation of a single nonspecular reflection is adequate, the transmission is a simple function: $W_{tr}(\mathscr{L}) = (1 - g\mathscr{L})$. In a glass neutron guide with walls polished to 14-th accuracy class and covered with nickel, the experimentally measured transmission[33] was 70% for $\mathscr{L} = 100$. This means that in such a neutron guide specular reflection takes place with probability 99.7%, i.e., the nonspecularity is ~0.3%.

It is interesting to compare this figure with the probability of nonspecular UCN reflection by the glass FLOAT, which was estimated in Ref. 34 at about 1–2%.

When g is determined from the transmission of neutron guides, there is some uncertainty depending on how the experiment is arranged. The point is that the transmission of a neutron guide of length $\Delta\mathscr{L}$ is measured by attaching to its exit another neutron guide of length $\mathscr{L}$. The transmission $W_{tr}(\Delta\mathscr{L})$ is determined as the ratio $J(\mathscr{L}+\Delta\mathscr{L})/J(\mathscr{L})$ and depends strongly on the transmission $W_{tr}(\mathscr{L})$ of the main neutron guide. If $W_{tr}(\mathscr{L}) \to 0$, then $W_{tr}(\Delta\mathscr{L}) \to 1$. But $W_{tr}(\mathscr{L})$ is unknown. We would encounter a similar uncertainty in electric circuits if we were to determine the resistance from the change in the current, knowing neither the emf nor the resistance of the source.

To reduce the uncertainty, it is necessary to use a monitor to establish the change in the flux at the entrance when the investigated section is added. An uncertainty always arises because the added section partly reflects the neutrons back into the main neutron guide, where, after diffuse reflection on the walls, they can return to the investigated section, effectively increasing the incident flux.

Besides straight neutron guides, it is of interest to study bent ones. If a neutron guide has one bend through angle α, then the transmission of the bend itself can be estimated as the ratio $W_{tr}(\alpha,\mathscr{L}_1,\mathscr{L}_2)/W_{tr}(\mathscr{L}_1+\mathscr{L}_2)$, where $W_{tr}(\alpha,\mathscr{L}_1,\mathscr{L}_2)$ is the transmission of the bent neutron guide. The experiments of Refs. 32 and 35 showed, for example, that a sharp 90° bend reduces the transmission by about 25%. A theoretical calculation[36] with purely specular reflection by the walls leads to the same result. It should be noted that in the presence of nonspecular reflection the resistance of the bend must, in general, depend on the lengths $\mathscr{L}_1$ and $\mathscr{L}_2$ of the straight sections. The longer these sections, the smaller must be the resistance of the bend. In particular, for $g = 1$ and $A(\Omega) = 1$ in the indicatrix (15) the transmission of the bend approaches unity already when the lengths of the arms are about 2.

Interesting experiments on neutron transport in an unsteady regime were made in Ref. 33. In these experiments, the neutron guide was covered by a screen at a certain distance from a detector, and the detector counting rate $J(t)$ was measured as a function of the time after the opening of the screen. The calculations of Ref. 37 show that from this experiment one can determine the nonspecularity parameter, the loss coefficient, and the average velocity of the ultracold neutrons in the neutron guide. The form of the dependence $J(t)$ is interesting. In some cases, it can exhibit a resonance-type peak.

Straight neutron guides transmit not only ultracold neutrons but also more energetic neutrons. To obtain a pure beam of ultracold neutrons, it is necessary to send the beam through a bent neutron guide. The "purification" is better, the greater the number of bends and the sharper they are. Thus, neutron guides are not only means of transport but also filters. It must, however, be remembered that the bends attenuate the UCN flux as well.

In principle, ultracold neutrons can be transported di-

rectly in a storage container.[38] In this case, the times at which the acceleration begins and ends are the most important, since the starting of an acceleration a is equivalent to the switching on of a "gravitational" field, and each neutron at distance z from the "bottom" of the container acquires an additional potential energy maz. In a container with maximal diameter 40 cm and $a = 1$ m/sec^2 at the maximal acquired energy is 4 neV.

3. EXPERIMENTAL APPARATUS

Detectors

The principles of detection of ultracold neutrons are the same as for thermal neutrons. Track, scintillation, and electric-discharge detectors are used. They are distinguished, first, by the fact that one needs little matter (radiator) to capture the neutrons, since the UCN velocity is low and the capture cross section increases in proportion to $1/v$. The amount of matter is chosen to make the probability of UCN capture near unity and the probability of detection of a thermal neutron small. Second, the potential barrier plays an important part. If the radiator is solid, as, for example, in a scintillation counter, the potential of the radiator itself is important. This potential must be sufficiently low, since otherwise it will reflect neutrons, and detection will occur with very low probability in a thin layer (about 10 nm). In gas counters, the potential of the window is important. The reflection by the detector can be reduced by the choice of the chemical or isotopic composition (for example, in Li scintillation detectors the radiator potential can be decreased by adding ^{7}Li). The reflection can also be reduced by moving the detector toward the neutrons, increasing thereby the neutron velocity relative to the detector. As an example, we may mention the scintillation detector in the form of a rotating plastic disk with a corrugated surface on which the scintillator is deposited.[39] Another example is a rotating cylindrical gas detector with a corrugated side surface.[40] The detector of Ref. 39 is nearly ideal, having almost unit efficiency in the entire range of UCN energies.

However, simpler and more reliable in use is the widely employed gas proportional detector with ^{3}He.[41]

The entrance window is made of aluminum foil about 100-μm thick. To prevent it reflecting the ultracold neutrons, the detector is lowered by about 50 cm. Then before detection the neutrons are accelerated by the gravitational field and readily pass the window. In Ref. 42, the detector window was made of a 12-μm titanium film, for which the potential is negative and the reflection less, though the cross section for neutron capture by titanium is 30 times higher than by aluminum. The gas counter is filled with ^{3}He and CO_2 (up to 5×10^2 Pa) and argon up to 10^5 Pa.

In track detectors, a mixture of ^{235}U and Ti is used[43] to lower the potential barrier. Other detectors, less widely used, are described in Ref. 44. In the experiment of Ref. 39, the spectral characteristics of some detectors were measured.

To measure the background, the entrance window of the detector is covered by a thin copper screen (5–10 μm). The number of detected ultracold neutrons is determined from the "screen difference," i.e., from the difference between the counts of the detector in the open and closed states. The more energetic neutrons also contribute to this screen difference if the normal component of their velocity relative to the screen is less than the limiting value. It is obvious that the contribution of the neutrons above the limit is greater, the higher the detector current in the closed state. In a purified beam of ultracold neutrons, the closed-detector current can be reduced to 5–10% of the UCN count.

UCN Spectrometers

For the spectrometry of ultracold neutrons one uses a gravitational field, since they have a low kinetic energy. In a gravitational spectrometer, the UCN energy is measured by means of a neutron-guide section that has a Π-shaped elbow. If the elbow is around a horizontal axis, then its horizontal part is raised or lowered. If it is raised by height H, neutrons whose kinetic energy to the left of the elbow is less than mgH, where m is the neutron mass, cannot overcome the gravitational barrier, i.e., they cannot pass to the right of the elbow. Thus, a detector situated to the right of the elbow detects only those ultracold neutrons whose energy is higher than mgH, i.e., the spectrometer is an integral spectrometer. If the elbow lowers through height H, the neutrons, accelerated in the gravitational field, acquire an additional kinetic energy mgH, and if to the left of the elbow their energy was greater than $E_{\rm lim} - mgH$, where $E_{\rm lim}$ is the critical energy of the walls of the elbow, then below it they are above the critical energy and can readily pass through the walls of the neutron guide. Thus, a rising elbow cuts off the spectrum below and a lowering elbow above.[27]

A differential spectrometer, which cuts out a line in the required part of the spectrum, can be constructed by means of two successive such elbows, one of which raises and the other lowers.[35] A variant is also possible[45] with one elbow. Its horizontal part has walls with low critical energy ΔE. In principle, such a spectrometer must pass only those neutrons that to its left have energy $mgH < E < mgH + \Delta E$. But in practice neutrons with energy greater than ΔE may not all pass through the walls as they pass along the horizontal part of the spectrometer, and therefore the resolution of the spectrometer is worse than ΔE.[46] The situation can be corrected if the neutrons are forced to remain in the spectrometer.[47]

The interpretation of the spectra obtained by means of gravitational spectrometers contains some uncertainties.

The change in the detector counting rate when the elbow in an integral spectrometer is turned depends not only on the measured spectrum but also on how rapidly the ultracold neutrons cross over and how rapidly the neutrons are detected by the detector.[47,48]

A time-of-flight spectrometer is more reliable from the point of view of interpretation but has lower luminosity.[49] However, it measures the distribution only with respect to one velocity component. If its measurements are to correspond to the distribution with respect to the total energy, it is necessary to use collimators, which strongly reduce the luminosity of the spectrometer. The use of the correlation method with stochastic modulation of the beam improves

the spectrometer luminosity.[50] Figure 1 shows the UCN spectrum in a channel obtained by a correlation spectrometer. Time-of-flight spectrometers are not restricted to ultracold neutrons. The only difference in the UCN case is the short—about 10 cm—flight path in horizontal channels and the need to take into account the influence of gravity on the flight time in vertical channels.

The ideal spectrum is the start of the Maxwellian spectrum $cEdE$. It is bounded below by the E_{lim} of the neutron guide. In practice, however, the spectrum begins to fall even before E_{lim}, since as E_{lim} is approached the coefficient of loss when the neutrons are reflected by the walls of the neutron guide increases sharply. In addition, the spectrum is depleted near $E \approx 0$ either because of the limiting energy of the converter or because of gravity, since the lower the neutron velocity, the more collisions it makes with the wall because of the parabolicity of the free-fall trajectory.

4. THEORY OF NEUTRON–MATTER POTENTIAL INTERACTION

Having considered the experimental means of studying ultracold neutrons, we now turn to the fundamental question of why they are reflected at all, and present the main ideas so far developed about the interaction of ultracold neutrons with matter.

Theory of Multiple Wave Scattering (Ref. 51)

The ideas here can be briefly summarized as follows. Reflection from matter is a process of multiple rescattering of the neutron wave by individual nuclei. This is a coherent process in which there is interference between the rescattered waves, and as a result of the interference the incident wave is transformed into a scattered wave of complicated structure amenable to exact calculation only in individual special cases. However, at low energies of the incident neutron, the main part of the scattered neutron field is concentrated in the specularly reflected wave and the refracted wave, and the amplitudes and phases of these waves are to a high accuracy the same as if the neutron–matter interaction were described by the potential $u_0 = (\hbar^2/2m)4\pi N_0 b$, where N_0 is the number of atoms per unit volume, b is the coherent scattering amplitude, and m is the neutron mass. In what follows, we shall omit the factor $\hbar^2/2m$ throughout. We emphasize that we are here dealing with a coherent wave process. In addition to it, there may be incoherent processes which may also lead to neutron reflection by matter, but to reflection of Albedo type.

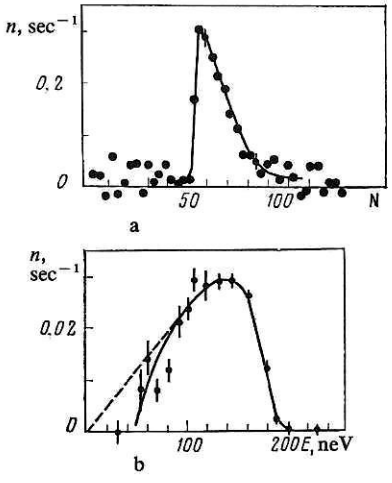

FIG. 1. Differential spectrum of ultracold neutrons at the exit of the neutron guide of the SM-2 reactor at the Scientific Research Institute of Atomic Reactors at Dimitrovgrad, measured by a correlation spectrometer with flight base of 31 cm: a) using the time of flight; b) after conversion to the energy.[50]

The potential u_0 can be positive,i.e., can lead to repulsion of a neutron by the matter, despite the interaction potential with each nucleus being negative. This is explained by the fact that the sign of the amplitude b can be, and in the majority of cases is, opposite to the sign of the nuclear potential.[144] To describe the interaction of a slow neutron with a nucleus, it is sufficient to know only b. Using this, we can replace the actual potential, as Fermi showed, by the pseudopotential $4\pi b\delta(r)$, where $\delta(r)$ is the Dirac δ function. At the same time, the potential u_0 can be represented as the average, over the volume of the matter, of the sum of the potentials of the individual nuclei:

$$u_0 = \left\langle \sum_i 4\pi b_i \delta(\mathbf{r} - \mathbf{r}_i) \right\rangle$$

$$= 4\pi \langle b_i \rangle N \int \theta(\mathbf{r}_i \in V)\, \delta(\mathbf{r} - \mathbf{r}_i)\, d\mathbf{r}_i / V, \tag{17}$$

where N is the total number of nuclei in the volume V of the matter, b_i is the amplitude for scattering by a nucleus at the point $\mathbf{r}_i$, and $\langle b_i \rangle = b$ is the coherent scattering amplitude. From the expression (17) we can, in particular, obtain the potential for a chain of atoms arranged along the z axis with linear density N_1, for the plane $z = 0$ containing atoms with two-dimensional density N_2, and for the half-space $z > 0$ containing three-dimensional density $N_3 = N_0$. The potentials in these three cases are, respectively,

$$4\pi b N_1 \delta(\mathbf{r}_\perp); \tag{18a}$$

$$4\pi b N_2 \delta(z); \tag{18b}$$

$$4\pi b N_0 \theta(z \geqslant 0), \tag{18c}$$

where $\mathbf{r}_\perp = (x, y)$. The averaging (17) leads to the correct expression for the matter potential, but cannot serve as a rigorous derivation of it. For a rigorous proof it would be necessary to solve exactly the scattering problem for a given set of nuclei and to compare the field of the scattered waves with scattering by the potential (17). Such a comparison would reveal the scattering features not contained within the approximation (17). However, in the general case it is not possible to solve the scattering problem exactly, and therefore the potential (17) can be rigorously justified only in individual special examples, namely, for a linear infinite periodic chain and for an infinite crystal plane. The solution for a semi-infinite crystal can be obtained completely only after replacement of each crystal plane by the potential (18b).

All the problems listed above can be solved by the method of multiple wave scattering. In this method, the neutron wave function is expressed as a sum of the incident wave and the scattered waves:

$$\Psi(\mathbf{r}) = \Psi_0(\mathbf{r}) - \sum_i b_i \psi_i G_0(\mathbf{r} - \mathbf{r}_i); \tag{19a}$$

$$G_0(\mathbf{r}) = \exp(ikr)/r, \tag{19b}$$

where $\Psi_0(\mathbf{r})$ is the wave function of the incident neutron, $G_0(\mathbf{r})$ is a scattered spherical wave, and the coefficients ψ_i represent the wave function at the position $\mathbf{r}_i$ of nucleus i. These coefficients are determined with allowance for scattering and rescattering and satisfy the system of algebraic equations

$$\psi_i = \Psi_0(\mathbf{r}_i) - \sum_{j \neq i} b_j \psi_j G_0(\mathbf{r}_i - \mathbf{r}_j). \tag{20}$$

Equations (19) and (20) form the basis of the theory of multiple wave scattering.

We consider first disordered matter. It is of course impossible to find the exact wave function, but one can find the averaged $\langle \Psi \rangle$, i.e., the coherent part. The averaging is over the positions of the atoms. It is most readily done in the case of completely disordered matter, in which each atom can be situated near any point $\mathbf{r}_i$ of the volume V with probability $d^3 r_i / V$, independently of the other atoms. Averaging of (19a) and (20) leads to the simultaneous integral equation

$$\langle \Psi(\mathbf{r}) \rangle = \Psi_0(\mathbf{r}) - \sum_i \langle b_i \rangle \int_V G_0(\mathbf{r} - r_i) \langle \psi(\mathbf{r}_i) \rangle \, d^3 r_i / V$$

$$= \Psi_0(r) - N_0 b \int_V G_0(\mathbf{r} - \mathbf{r}') \langle \Psi(\mathbf{r}') \rangle \, d^3 r'. \tag{21}$$

Applying to it the operator $\Delta + k^2$, we obtain the differential equation

$$(\Delta + k^2 - u_0 \theta(\mathbf{r} \in V)) \langle \Psi(\mathbf{r}) \rangle = 0, \tag{22}$$

from which it follows that the matter can be ascribed the potential $u_0 = 4\pi N_0 b$.

The scattering problem is solved exactly in the case of an infinite periodic chain and a plane in Refs. 52 and 53. We shall not give the solutions here but merely mention the main features of the exact wave functions. For $k < 2\pi/a$, where a is the period, the main part of the scattered field is formed by waves having amplitude and phase the same as for scattering by the potentials (18a) and (18b), respectively, except that the amplitude b in these expressions must be replaced by $\tilde{b}$:

$$\tilde{b} = b/(1 - ikb). \tag{23}$$

Besides them, the scattered field contains diffracted waves, which are then damped exponentially with increasing distance from the chain or plane. Thus, at a distance of the order of a period these waves can be ignored with high accuracy.

Using this result, we represent a crystal filling the half-space $z > 0$ as a set of crystal planes parallel to the surface of the crystal, each of them described by the potential (18b) with the amplitude (23) instead of b. Then the problem of scattering by such a crystal is reduced to a one-dimensional form with a Kronig–Penney potential. The solution can then be found exactly. The reflected field contains one specular wave with amplitude

$$r^+(k_\perp) = \frac{\sqrt{k_\perp + p \tan\varphi} - \sqrt{k_\perp - p \cot\varphi}}{\sqrt{k_\perp + p \tan\varphi} + \sqrt{k_\perp - p \cot\varphi}}, \tag{24}$$

where $p = 2\pi N_2 \tilde{b}$, $\varphi = k_\perp a/2$, and $k_\perp$ is the component of the wave vector of the incident neutron normal to the surface of the crystal. For $k_\perp a \ll 1$, the expression (24) can be reduced, to terms of order $(k_\perp a)^2$, to the form

$$r^+(k_\perp) = (k_\perp - k'_\perp)/(k_\perp + k'_\perp), \quad k'_\perp = \sqrt{k_\perp^2 - u_0}, \tag{25}$$

which is characteristic for reflection by a potential step of height $u_0 = 4\pi N_0 \tilde{b}$. Thus, the potential is indeed equal to (18c) with the only change relating to the replacement of the amplitude b by $\tilde{b}$ (23). For $k_\perp^2 < u_0$, we have $k'_\perp = i\sqrt{u_0 - k_\perp^2}$, and $r^+(k_\perp)$ can be represented in the form

$$r^+(k_\perp) = \exp(-2i\varphi), \quad \varphi = \tan^{-1}(k_\perp/\sqrt{u_0^2 - k_\perp^2})$$

$$= \cos^{-1}(k_\perp/\sqrt{u_0}), \tag{26}$$

and for real u_0 there is total reflection, since $|r^+(k_\perp)|^2 = 1$.

Before we go further, it is worth reproducing some compact and as yet little known expressions for scattering by a periodic potential obtained in connection with the investigation of UCN interaction with matter,[54,55] but of more general application. The amplitude of reflection from an arbitrary semi-infinite periodic potential can be expressed in the form

$$R_\infty = \frac{\sqrt{(r+1)^2 - t^2} - \sqrt{(r-1)^2 - t^2}}{\sqrt{(r+1)^2 - t^2} + \sqrt{(r-1)^2 - t^2}}, \tag{27}$$

where r and t are the amplitudes of reflection and transmission of one period. In particular, in the case of the Kronig–Penney potential

$$r = p \exp(2i\varphi)/(ik_\perp - p); \tag{28a}$$

$$t = ik_\perp \exp(2i\varphi)/(ik_\perp - p), \tag{28b}$$

where $\varphi = k_\perp d$, d being the period.

If a periodic potential is not infinite but has finite length (i.e., a finite number of periods), then the scattering by it can be described, with allowance for (27), in the same way as by a rectangular barrier of width l. If the amplitudes of the reflected and transmitted waves are denoted by R_l and T_l, respectively, then

$$R_l = R_\infty \frac{1 - \exp(2iql)}{1 - R_\infty^2 \exp(2iql)}; \tag{29a}$$

$$T_l = \exp(iql) \frac{1 - R_\infty^2}{1 - R_\infty^2 \exp(2iql)}, \tag{29b}$$

where q is the quasimomentum of the neutron within the region occupied by the potential. It is determined by the expression

$$\exp(iql) = (\sqrt{(t+1)^2 - r^2}$$

$$- \sqrt{(t-1)^2 - r^2})/(\sqrt{(t+1)^2 - r^2} + \sqrt{(t-1)^2 - r^2}). \tag{30}$$

Equations (27)–(30) contain all expressions relating to the dynamical theory of diffraction by an ideal single crystal.

We now turn to ultracold neutrons. The quantity u_0 determines the critical energy E_{lim} of the matter. In accordance with (26), total reflection occurs at all angles of incidence if $k^2 < E_{\text{lim}}$. The critical energy E_{lim} is different for different materials, but does not exceed the level 2.5×10^{-7} eV. To it there corresponds a critical velocity v_{lim} such that storing is possible for a given material only when $v < v_{\text{lim}}$. For copper, $v_{\text{lim}} = 5.7$ m/sec; for Al, $v_{\text{lim}} = 3.2$ m/sec, and for Be, $v_{\text{lim}} = 6.8$ m/sec.

Within the matter the wave function is damped expon-

entially; the penetration depth into the matter is different for different materials and neutron energies, but on the average it can be estimated at $l = 1/\sqrt{u_0 - k^2} \approx 1/\sqrt{u_0} \approx 10$ nm.

Loss Coefficient

The total reflection of ultracold neutrons is not in reality absolutely total, since on reflection there is a loss of the ultracold neutrons with a small probability μ, this being different for different materials but lying in the majority of cases in the range $\mu \approx 10^{-3}$–10^{-5}. We shall now show how the loss coefficient μ can be found.

In general, the amplitude b has an imaginary part; accordingly, the potential has one too: $u_0 = u_0' - iu_0''$. Therefore, the phase of the reflected wave also has an imaginary part: $\varphi = \varphi' - i\varphi''$. If $u_0'' \ll u_0'$, which is generally the case, then $\varphi'' \approx u_0''(\partial\varphi/\partial u_0)$ and the reflection coefficient differs from unity by the amount

$$\left.\begin{aligned} &\mu = 1 - |\, r^+(k_\perp)\,|^2 = 1 - \exp(4\varphi'') \approx 4\varphi'' = 2(k_\perp/k_\perp'')\,\eta; \\ &k_\perp'' = \sqrt{u_0 - k_\perp^2}; \quad \eta = u_0''/u_0'. \end{aligned}\right\} \tag{31}$$

The imaginary part $b = b' - ib''$ is determined by the optical theorem: $b'' = k\sigma_t/4\pi$, where σ_t is the total cross section, including the absorption cross section σ_a and the elastic-scattering cross section $\sigma_{el} = 4\pi|b|^2$. Therefore, in the case of reflection by disordered matter, for which $u_0 = 4\pi N_0 b$, the attenuation of the specularly reflected wave compared with the incident wave—it is described by the coefficient (31)—can be explained by the losses due to capture by the nuclei of the matter and elastic scattering. But in a trap surrounded by such walls there should be no loss of neutrons in the absence of capture ($\sigma_a = 0$). It follows that the cross section of elastic scattering does not lead to losses but describes nonspecular reflection. In the case of reflection by ordered matter, the interaction potential $u_0 = 4\pi N_0 \tilde{b}$, and the imaginary part of the amplitude $\tilde{b}$ does not contain σ_{el} (23) at all, and therefore the coefficient μ describes only the absorption loss. Thus, when neutrons are stored in a container, every collision with the wall is accompanied by a loss, which can be described by the loss coefficient μ with $\eta = k\sigma_a/4\pi b'$.

Hitherto, we have considered reflection from matter with nuclei fixed rigidly in their positions. In reality, the atoms execute thermal vibrations, and this leads to inelastic scattering, in particular to a neutron being heated with a certain probability as a result of collision with the wall to an energy above E_{lim} and leaving the trap. This process must also lead to losses of ultracold neutrons in traps. A detailed investigation[56,57] shows that the cross section σ_{ie} of inelastic scattering occurs in the loss coefficient on an equal footing with σ_a, i.e., $\eta = k(\sigma_a + \sigma_{ie})/4\pi b'$.

Inelastic scattering leads not only to the cross section σ_{ie}, but also to the Debye–Waller factor $W_D = \exp(-q^2\langle\xi^2\rangle)$, where q is the momentum transfer and $\langle\xi^2\rangle$ is the mean-square amplitude of the atomic vibrations. This factor has the effect of reducing the elastic-scattering amplitude b. In the calculation of the refraction coefficient, the factor W_D plays no part, since in this case it is necessary to know the amplitude of scattering through zero angle, at which $q = 0$. However, reflection is accompanied by a nonzero q. In the case of total reflection $q = 2ik_\perp''$, and therefore the phase of the reflected wave contains not the potential u_0 but the somewhat larger potential $u_0 \exp[2(u_0 - k_\perp^2)\langle\xi^2\rangle]$. However, the critical energy E_{lim} is not changed by this, since for $k_\perp^2 = u_0$ the additional factor becomes unity. For $k_\perp^2 > u_0$, this factor becomes less than unity, and the effective potential energy and, hence, the reflection coefficient are slightly reduced. The change in the phase of the reflected wave for $k_\perp^2 < u_0$ is due to the fact that the thermal motion of the atoms smears the interface over a distance of the order of the vibration amplitude.

5. STORAGE OF NEUTRONS IN CONTAINERS

Connection Between the Storage Time τ and the Loss Coefficient μ

The storage time of neutrons in a container is limited, first, by the neutron lifetime $\tau_\beta \approx 1000$ sec and, second, by losses occurring when there are collisions with the wall. For neutrons with given velocity v,

$$N(v,\ t) = N(v,\ 0)\exp(-t/\tau), \quad 1/\tau = 1/\tau_\beta + 1/\tau_l, \tag{32}$$

where τ_l is the storage time without allowance for decay: $\tau_l = t_f/\mu$; t_f is the average time of free flight between two collisions with the walls: $t_f = l_f/v$; l_f is the mean free path between collisions: $l_f = 4V/S$; V is the volume of the container; and S is the surface area of its walls. The loss coefficient μ is averaged over the angles of incidence under the assumption of an isotropic distribution of the neutrons within the container:

$$\left.\begin{aligned} &\bar{\mu} = \int \mu(k_\perp)\cos\theta\, d\Omega/\pi = (2\eta/y^2)\left(\sin^{-1} y - y\sqrt{1-y^2}\right), \\ &y = v/v_{lim}. \end{aligned}\right\} \tag{33}$$

The dependence (32) is exponential, but since the spectrum of the neutrons stored in the container is fairly broad, the dependence of the total number of neutrons in the container on the time, $N(t)$, is nonexponential. Figure 2 shows one of

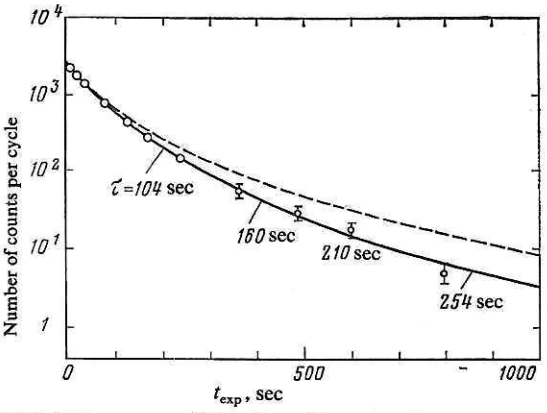

FIG. 2. Storage curve[58] for ultracold neutrons in a copper container purified by an argon glow discharge. For exponential decrease, the curve would have the form of a straight line. In the present case, the slope decreases with the time, since the faster neutrons perish more rapidly. The average velocity of the neutrons confined in the trap varies from 4.5 m/sec at $t = 0$ to 1.9 m/sec at $t = 800$ sec. The continuous curve corresponds to the theory with loss coefficient increased by a factor of three, and the broken curve is obtained with neglect of the intrinsic decay.

the storage curves, i.e., the dependence $N(t)$ obtained for neutrons stored in a copper container.[58] Since it is the faster neutrons that perish more rapidly as a result of collisions with the walls, the UCN spectrum in a container becomes softer with time, and the time τ_1, and hence τ, increases. It is clear from the figure that it is not convenient to characterize storage of ultracold neutrons by the time τ, since it depends on the geometrical dimensions of the container and on the velocity v. It is better to use the coefficient $\eta = k\sigma_1/4\pi b$, which depends only on the properties of the material of the container walls. Since the loss cross section $\sigma_1 = \sigma_a + \sigma_{ie}$ at low velocities behaves as $1/k$, the quantities $k\sigma_1$ and η do not depend on the energy, and to estimate η we can use the cross sections taken at the thermal point, i.e., at the velocity 2200 m/sec, or wavelength 0.18 nm. In the case of copper, the main contribution to the cross section σ_1 is made by absorption, $\sigma_a = 3.77$ b, whereas $\sigma_{ie} = 0.15$ b,[59] where 1 b $= 10^{-24}$ cm^2. Thus, $\eta = 1.45\times10^{-4}$. The experimental curve in Fig. 2 corresponds to an η twice as large. In the case of weakly absorbing materials, for example, Be, η should be at the level 5×10^{-6}, but experiments led to a value almost two orders of magnitude larger. This discrepancy between theory and experiment presented a problem that has not yet been completely resolved. We shall show in what follows the directions in which experimental and theoretical searchers have been made.

First Experiments on UCN Storage

The possibility of prolonged storage of neutrons is the main feature of ultracold neutrons making it possible to use them to solve a number of physical problems. It is therefore necessary to achieve the maximal storage time. Storage experiments are also interesting in their own right, since the neutrons stored in a container represent a distinctive nonequilibrium ideal quantum gas with which a temperature $\sim10^{-3}$ °K can be nominally associated.

The experiments are as follows. Neutrons are fed into a container, which is then closed and kept in the closed state for the time t_{exp}, after which it is opened and the neutrons remaining in it travel to the detector. The dependence $N(t_{exp})$ of the detector count on the delay (exposure) time t_{exp} is called the storage curve. Figure 3 shows the arrangement of the first experiment and its results. We have plotted not only the storage curves (Fig. 3c) but also the "outflow" curve (Fig. 3b), which shows how the detector count depends on the time after the exit is opened. From the outflow curve one can find the average velocity of the neutrons remaining in the container, and from the storage curve the average storage time, from which the average loss coefficient can be determined. In the given case, the experimentally deduced coefficient η for chemically polished copper is approximately 5×10^{-4}, and for pyrographite it is about 15×10^{-4}, whereas it should be 1.45×10^{-4} and 0.02×10^{-4}, respectively. There is a strong discrepancy between the experiment and theory, especially in the latter case. A similar strong discrepancy was found for beryllium and glass. Agreement between theory and experiment was observed only for storage in a container made of boric glass,[28] in which the storage time must

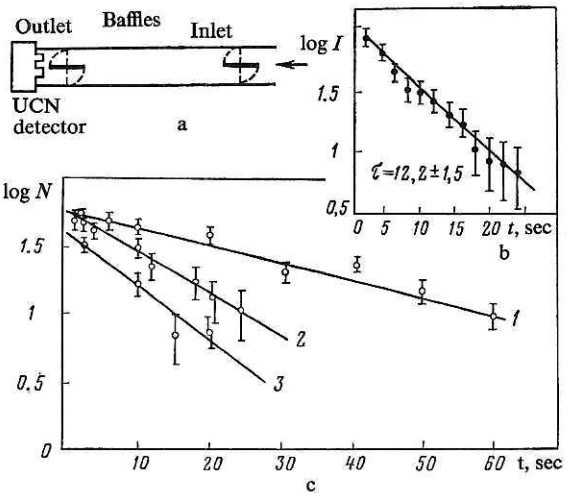

FIG. 3. Measurement of storage time in a container (diameter 14 cm, length 174 cm) (a) and its results: b) "outflow" curve; c) storage curves. 1) Chemically polished copper tube, average storage time 33 sec; 2) untreated copper foil, $\tau = 14$ sec; 3) pyrographite, $\tau = 11$ sec.

be short because of capture by boron. It is interesting that for all the investigated materials the coefficient η is approximately at the same level 10^{-3} for different surface treatments. Attempts were made to find a variation of the coefficient η with the temperature. Attempts with copper at 250 °C and graphite at -190 °C did not reveal any significant difference.[27] In the experiment of Ref. 33, UCN storage in a nickel container (nickel deposited on a glass surface) was investigated. Prolonged heating of the container at 150 °C and measurement of the storage time at room temperature, and also at 200 °C also did not reveal any change in the coefficient η, which exceeded the theoretical value by 4–5 times.

In the experiment of Ref. 60, storage in a boron-free glass container was investigated. It was found that a change in the temperature of the container in the range 100–180 °K did not affect the storage time. A shortcoming of this experiment was that the temperature was distributed nonuniformly along the container and the spectrum of stored neutrons contained a part above the critical energy, so that a temperature effect could in principle be masked.

Attempts to Explain the Excess Loss Theoretically

Numerous suggestions were made to explain the results. In principle, rapid loss of the ultracold neutrons could be explained by the presence of cracks. It is true that estimates showed that cracks should not play an important part, but it was necessary to show this experimentally. To this end, cracks were varied in the experiment of Ref. 61 in a fairly wide range, but this hardly affected the storage time. The next, rather natural suggestion was the presence of contamination on the surface of the walls. The contamination could be of two types, leading to absorption of neutrons or heating of them. Absorbing contamination appears improbable, because there are few strongly absorbing substances in nature and they occur seldom. The most common is chlorine with a capture cross section 32.5 b for neutrons of velocity 2200 m/sec. Let us consider how much chlorine would have to be on the surface or in the surface region to explain the

anomaly in copper. The experimental value of η in copper is approximately twice the theoretical. This means that the loss cross section is twice the capture cross section in copper. Since $\sigma_a = 3.77$ b for copper, to explain the anomaly it would be necessary to assume that the contamination introduces additionally about 8 b. If the reason for the loss is chlorine, it would have to be present in the surface layer to a depth of 10 nm to the amount of one chlorine atom for four copper atoms. Such an amount is improbable in view of the negligible abundance of chlorine in the atmosphere. However, these arguments cannot be regarded as proof and require experimental verification, which will be discussed later.

It seems more natural to assume the presence of hydrogen-containing contamination. The cross section for inelastic scattering by bound hydrogen can be very large (80 b), and to explain the anomaly in copper it is sufficient to assume the presence of less than one hydrogen atom for 10 copper atoms in the surface layer of 10 nm. In principle, hydrogen-bearing substances cold also form films on the surface, and since the coherent amplitude of scattering on hydrogen is negative, the potential of the film–neutron interaction could be negative, i.e., there could be bound states within the film. However, for the formation of the first bound state the film thickness would have to be rather large. In the case of water, for example, the first bound state arises at film thickness 40 nm. Since the bound state relates only to the neutron motion perpendicular to the surface of the wall, a neutron could go over to the state as a result of scattering by elements of roughness increasing the momentum along the surface. But the elements of roughness also lead to the opposite scattering, i.e., to a neutron leaving the bound state. It should also be said that the possibility of binding has little influence on the neutron loss, which in any case is large for such a thick film.

All these processes are described here because they are interesting in their own right, but they cast little light on the anomaly in UCN storage, since thick films must evaporate on heating. The suggestion of hydrogen within the material also appears to be without foundation at the first examination, since inelastic scattering depends on the temperature (there are grounds for assuming that this dependence is not weaker than linear) but the experiments showed no such dependence.

It could be that the calculation of the inelastic-scattering cross sections does not take into account fully the fact of total reflection of the neutron, which changes the neutron wave function or does not take into account the change in the phonon wave function due to the presence of an interface. However, as is shown in Ref. 56, all these factors lead merely to a small correction to the loss coefficient. In Ref. 62, attention was also drawn to Rayleigh surface waves. Scattering by a Rayleigh wave can be described as diffraction by a static lattice if one goes over to a frame moving with the traveling wave, in which an ultracold neutron is represented by a thermal neutron. However, this diffraction contains the small factor $(a/l)^2 \approx 10^{-4}$, where a, the amplitude of the wave, is about 10^{-8} cm, and $l = 1/\sqrt{u_0}$ is the depth of neutron penetration into the matter in the case of total reflection: $l \approx 10^{-6}$ cm. In Ref. 56, it was shown that the Rayleigh wave gives only a small correction to the loss coefficient. In addition, scattering by surface waves must also depend on the temperature.

One further inelastic process is associated with acoustics.[63] Here, one really could expect additional losses that are more or less the same for all substances and do not depend on the temperature. Acoustic vibrations are characterized by a wavelength fairly long compared with the neutron wavelength, and therefore they lead to a quivering of the surface that for an ultracold neutron can be represented as motion of the matter as a whole. If the vibration amplitude is a and the frequency ω, then the surface moves with velocity $u = a\omega$. If $u \ll v_{\text{lim}}$, then the wall jolts the neutron and can either accelerate or decelerate it, depending on the phase of the vibration at which the collision with the wall takes place. Thus, the change in the neutron velocity can be described by a random process in which the neutron energy changes by $mu^2/2$ on the average in each collision. Once the total energy exceeds the critical energy, the neutron leaves the container with a high probability. A coefficient $\eta \approx 10^{-3}$ corresponds to about 1000 collisions with the container walls before an ultracold neutron reaches the energy E_{lim}. Accordingly, $mu^2/2$ must be $(E_{\text{lim}}/1000) \approx 10^{-10}$ eV, which corresponds to a velocity $u \approx 10$ cm/sec. At frequency $\omega \approx 10^6$ sec^{-1}, the amplitude must be 0.1 μm. The corresponding acoustic energy density $\rho u^2 \approx 10^{-5}$ J/cm^3 is extremely high compared with the characteristic acoustic unit 10^{-19} J/cm^3, which corresponds to noise of 140 dB. One could also imagine acoustic vibrations that after one collision heat a neutron with a certain probability to an energy just above the critical energy if a vibration quantum $\hbar\omega > E_{\text{lim}}$ is absorbed in a collision with a wall. Unfortunately, in this case too it is necessary to assume a very high acoustic energy density. The possibility of acoustic heating was also tested experimentally, and a negative result was obtained.[64,65]

In principle, the anomaly can also be explained by roughness of the surface. It all the dimensions of the elements of roughness are large, this leads to an increase in the total area S of the surface of the walls[66] and to a decrease in the mean free path $l = 4V/S$ compared with $l_0 = 4V/S_0$, where S_0 is the apparent surface of the walls. Thus, in determining η we may not take into account the factor $S/S_0 > 1$. If the height a of the elements of roughness is large, and the transverse dimensions small, it can be assumed that the interface is smeared over a depth of order a. In the case of reflection by a smeared interface, the neutron is decelerated as it approaches the wall and interacts with nuclei longer than in the case of reflection by a sharp boundary, which increases the loss coefficient. For $a \gg l = 1/\sqrt{u_0}$, the coefficient η increases in proportion to a/l and can become arbitrarily large.[67,68] However, the roughness equally increases the absorption and heating of the ultracold neutrons. Therefore, if the roughness is approximately the same for all substances, the storage times should differ as strongly as the theoretical values of η. This was not observed experimentally.

The situation is similar if we attempt to explain the increase in the loss coefficient by porosity of the material near the surface. In a sufficiently large pore (of radius $r > 10$ nm), a bound state can be formed.[69] This bound state decays either through loss in the four walls or by tunneling out of the pore. The tunnel effect has the consequence that the loss coefficient in the presence of a pore at depth H from the surface can increase[70] by $\exp(2H\sqrt{u_0})$ times if the energy of the incident neutron is near the energy of the bound state. However, once again the absorption and heating increase equally for all materials.

Attempts were made to explain the anomaly by fundamental reasons. It could be that we do not take into account correctly multiple scattering and rescattering of the waves. In Ref. 71 it was noted that the imaginary part of the scattering amplitude in the case of ultracold neutrons may be much larger than follows from the elementary theory of multiple wave scattering. However, no quantitative estimates were made.

In Ref. 72 it was suggested that the neutron is a nonspreading wave packet and with probability proportional to the fraction of waves in the packet with energy above the critical energy passes freely through the container walls. After interaction with the wall, the neutron re-establishes its packet structure.

In Ref. 73 it was suggested that a neutron can be in two different states (see also Ref. 30) differing by the value of an as yet unknown quantum number "crypticity." In these states, it interacts differently with matter. Assuming further some universal cypticity-nonconserving interaction, one can force the electron to oscillate between these states. On striking the wall, the neutron may be in the state in which it penetrates readily through the matter, which would be manifested as an increase in the loss coefficient.

Investigation of Heating of Ultracold Neutrons on Container Walls

To settle, once and for all, what happens—absorption or heating—to neutrons that disappear from a container, and experiment was made[74] in which a container with ultracold neutrons was surrounded by thermal neutron counters (Fig. 4). If the ultracold neutrons are heated when they collide with the wall, the counters at the periphery should detect this. The time dependence of the counting rate of the peripheral detectors should repeat the storage curve, and the total number of counted neutrons should be equal to the loss of ultracold neutrons during the time the container is kept in the closed state. This is in fact what happened. An experiment with an electrolytically polished copper container showed that the entire anomaly can be attributed to inelastic scattering. This result revived the hydrogen hypothesis. At about the same time a method was developed for determining the profile of the hydrogen distribution near the surface by means of the $p(^{15}N^{+},\gamma)^{16}O$ nuclear reaction. Measurement of the hydrogen abundance in electrolytically polished copper, graphite, and glass[75] showed that in a surface layer about 10-nm thick there are about 10^{16} hydrogen atoms per 1 cm^2. This means that every tenth atom is a hydrogen atom.

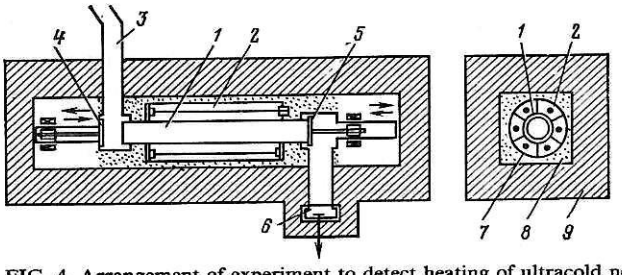

FIG. 4. Arrangement of experiment to detect heating of ultracold neutrons: 1) storage chamber; 2) peripheral counters; 3) UCN channel; 4) inlet valve; 5) outlet valve; 6) UCN detector; 7) 1.5-mm cadmium shield; 8) B_4C; 9) (CH_2) + B shield.[74]

Thus, everything seemed to be clear. Hydrogen was the culprit responsible for the short UCN storage time. It is easy to calculate that for $\sigma_{ie} \approx 80$ b an excess coefficient $\Delta\eta = 4\times10^{-4}$ requires $(v_{lim}/4.4)\times10^{16}$ cm^{-2} of hydrogen, v_{lim} being the critical velocity of the material in m/sec. But then why no temperature dependence? Could the anomaly be in fact a weak temperature dependence? In this connection, two theoretical models were considered. In one,[76,77] it was assumed that the hydrogen is bound strongly to the surface for motion along the normal but is almost free in motion along it. Such a model leads to a comparatively weak temperature dependence: $\eta \sim \sqrt{T}$. In the other variant the hydrogen has two closely spaced levels separated by $\Delta E \approx 10$ meV. Then down to the temperature 80 °K the population of the upper level and the inelastic-scattering cross section are almost independent of the temperature, while below 80 °K the cross section and, hence, η decrease with the temperature exponentially.[78] The exponential dependence can be made smoother if it is assumed that the distance ΔE between the levels varies from atom to atom, i.e., is smeared in accordance with some distribution.[79]

The first conjecture has the consequence that the energy of the heated neutron must be thermal, whereas the second conjecture has the consequence that the energy must be equal to the distance between the levels, i.e., about 10 meV. We note here that the lower the energy transferred to the neutron, the smaller the inelastic cross section and the more hydrogen that is needed to explain the anomaly. In the case of the first conjecture, the cross section for scattering by free hydrogen is four times less than by bound hydrogen, and therefore four times as much hydrogen is needed than would be the case for bound hydrogen.

In general, one can construct a model in which inelastic scattering is large without any hydrogen.[80] For this, one must suppose that the entire surface region of the material is divided into clusters with n atoms in each. If the scattering on a cluster occurs coherently, then its scattering amplitude is nb, where b is the amplitude for one nucleus, and the cross section is proportional to n^2b^2, i.e., n^2 times greater than for a single atom. But since the probability of inelastic scattering is proportional to the number of clusters, and this number is n times smaller than the number of nuclei, and is inversely proportional to the cluster mass, which is n times greater than the mass of a nucleus, it would appear that the n^2 gain is reduced to nothing. Nevertheless, one can still contrive to

obtain a gain. We note that the cross section for inelastic scattering by a free nucleus is inversely proportional, not to the mass M, but to $\sqrt{M}$. If we assume that the clusters vibrate independently of each other with very low frequencies, then inelastic scattering is accompanied by a transfer of many vibrational quanta, i.e., as if it occurred on a free particle. Therefore, in the denominator of the expression for inelastic scattering there is also a root of the mass, and overall clusters of n atoms lead to a probability of inelastic scattering that is $\sqrt{n}$ times greater than in the case of a uniform distribution of nuclei in the surface region. Of course, such a model is rather artificial.

Attempts to Eliminate Hydrogen

Since hydrogen was nevertheless detected, the question arose of its elimination or neutralization of its influence. One could attempt either to degas the walls or cover the hydrogen, or to replace it by deuterium. At first, an attempt was made to cover the hydrogen by a freshly deposited material.[81] For this, vaporizing elements were placed under the lid of a container (Fig. 5), and the container itself was raised relative to the level of the neutron guide by a height such that the neutrons filling it were kept by the gravitational field at the bottom of the container. The storage was done either at the time of deposition (in a dynamical regime) or immediately after deposition, the deposition being done at such a rate that hydrogen from the residual atmosphere could not contaminate the surface during the deposition. It was found that the storage time in aluminum, for example, does not depend on the deposition regime and is about 230 sec, whereas the storage time in an aluminum vessel that had simply been etched in NaOH and washed in distilled water the storage time was 170 sec. It is interesting that the storage time was about 650 sec in a beryllium-deposited container.

It is here necessary to make a small digression. Earlier, when the containers were tubes of diameter about 10 cm and length 1–3 m, the storage time, including storage in beryllium, was about 30 sec. It would seem that great progress is now observed. However, the previously stored neutrons had a fairly broad spectrum in the region of ultracold neutrons, whereas in the experiments of Ref. 81 they had an energy near 19 neV. In the earlier calculation of the loss coefficient η gravitation was not taken into account, since 100-neV neutrons can rise to a height of 1 m. In the determination of η, gravitation must now be taken into account. The storage time τ_1 due to losses in the walls (the loss time) can be represented in the form $\tau_1 = t_f/\mu$, where t_f is the time of flight between two collisions with a wall, and μ is the loss coefficient, which at low neutron velocities can be represented in the form $\mu = 2k_\perp \eta/\sqrt{u_0}$. Suppose for simplicity that the ultracold neutrons are kept on an infinite plane; then it follows from elementary physics that $t_f = 2v_\perp/g$, where $v_\perp$ is the velocity component normal to the plane and g is the acceleration of free fall. We then obtain the expression $\tau_1 = v_{\lim}/\eta g$. If from the experimental storage time we now subtract the intrinsic neutron lifetime, we obtain $\eta = 2\times 10^{-4}$ in beryllium. Thus, the anomaly persists at the previous level. Similar values of η were also obtained when CO_2 and D_2O were frozen onto the container walls at liquid-nitrogen temperature. This means that either the hydrogen cannot be eliminated by depositing a new film or the anomaly is still not explained by hydrogen.

In Ref. 82, small copper samples were purified by ion bombardment with a simultaneous measurement of the hydrogen content. It was found that the amount of hydrogen can be reduced to the level 3×10^{15} cm^{-2}, but still the value of η determined from storage experiments in copper containers purified by ion bombardment (see Fig. 2) led to twice the theoretical value.

An attempt to replace hydrogen by deuterium was made in Refs. 81 and 83. In both cases the attempt was unsuccessful, but this does not mean that there was no hydro-

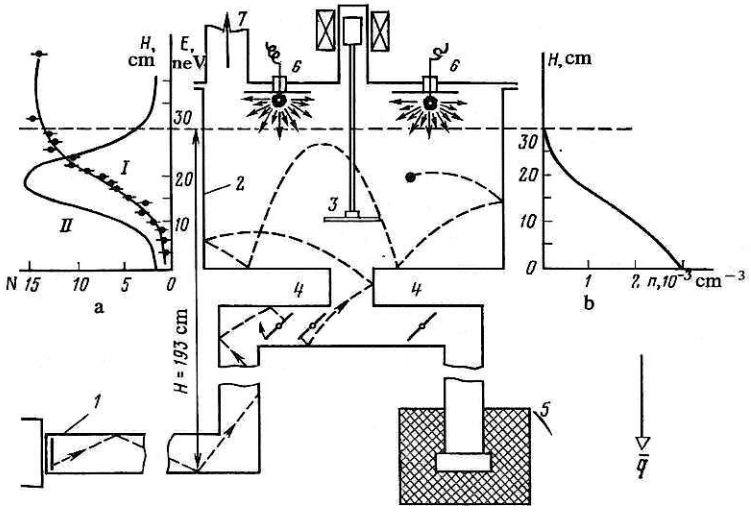

FIG. 5. Arrangement of experiment for storage in a container with walls with deposited coverings: 1) neutron guide; 2) storage chamber; 3) inlet and outlet valve; 4) distributive baffles; 5) detector; 6) metal vaporizers; 7) exit to vacuum system. The broken curve shows the imagined trajectory of a neutron.[81] The left-hand insert (a) shows the integrated spectrum (I) and a Gaussian differential spectrum fitted to it (II). The right-hand insert (b) shows the distribution of the neutrons over the height of the container.

gen, since the failure could be due to the incorrect technology of isotopic substitution, the efficiency of which was not measured.

Recent Achievements in Storing Ultracold Neutrons

Other attempts have been made to deuterate, the hydrogen content being measured by ion beams.[84,85] The deuteration was done either by boiling in D_2O or by etching in DF for 15 min. However, these methods did not reduce significantly the amount of hydrogen on the surface. Beams of $^{15}N^+$ or ^{11}B ions were also used to measure the amount of hydrogen in other treatments of the surface: annealing at high temperature, deposition of fresh metal, and purification of the surface by ion bombardment. The change in the hydrogen content on the surface as a result of the influence of the residual vacuum or after exposure of the surface in atmospheric air or hydrogen was also investigated.[85,84] It was found, for example, that when nickel is heated to 1000 °C the amount of hydrogen on the surface is reduced to 10^{14} cm^{-2} in a layer of about 20 nm, but in a vacuum of 10^{-4} Pa the hydrogen content increases during 2–3 h to $(4–5)\times10^{15}$ cm^{-2}. Heating of nickel to only 150 °C also purifies the surface fairly well, and this purity is maintained for a day if the residual vacuum is 10^{-7} Pa. A lead film freshly deposited at the rate of 7 monolayers per second in a vacuum of 10^{-4} Pa contains about 5×10^{15} cm^{-2} of hydrogen, but in 1 h this amount increases by a factor of almost two. For aluminum and approximately the same rate of deposition one can reduce the amount of hydrogen to 10^{15} cm^{-2}, but in a vacuum of 10^{-4} Pa this amount increases during 1 h to 3×10^{15} cm^{-2}. By ion bombardment one can reduce the amount of hydrogen on the surface of copper or stainless steel to a level below 5×10^{15} cm^{-2}.

Ion purification is fairly effective, since it purifies only the surface layer without strongly heating the material. This makes it difficult for hydrogen to diffuse to the surface from deeper layers. In Ref. 85, a study was made of UCN storage in containers whose walls were purified by a glow discharge in an atmosphere of argon or deuterium. Figure 6 shows the storage curves in a quartz container after different treatments of the surface. Also plotted is the curve calculated for the theoretical value $\eta = 10^{-5}$ for quartz and $\eta = 10^{-4}$ for two stainless steel valves. In addition, and this is an important point, the calculation included a further parameter—the width of the possible gap between the valves and the quartz walls. The width of the gap was taken to be 10^{-3} cm. The loss coefficient η calculated using the storage curve 6 exceeds the theoretical value by only three times.

It would seem that this experiment brings us to the final solution to the problem of UCN storage, but there are numerous points that prevent us taking this conclusion as unconditional. Above all, the spectrum of the neutrons stored in the container is not known. In the calculation it was assumed to be Maxwellian, but if it is softer, then the loss coefficients obtained in the study would be much too low. Further, the gap width ε was chosen rather arbitrarily, and this has a strong influence on the determination of η. Note that allowance for the gap width in the loss coefficient can be

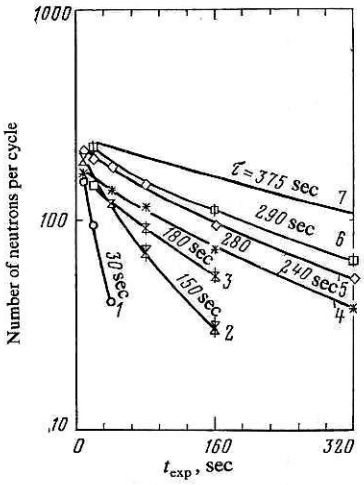

FIG. 6. Storage curves in a horizontal quartz container (diameter 6.4 cm, length 1 m) with two stainless steel valves at the ends in the case of different treatments of the surface of the walls: 1) washing with alcohol; 2) ultrasonic purification with detergent and washing with distilled water; 3) purification by a discharge, exposure 2 days, in atmosphere and procedure 2; 4) discharge in an atmosphere of 80% Ar + 20% D_2 for 30 min; 5) the same, purification by discharge with a large admixture of D_2O; 6) purification by discharge as for curve 3 but with the addition of deuterated methylalcohol vapor; 7) calculated curve for an ideal surface.[85]

put in the form $\Delta\eta = (\varepsilon/l)(v_{lim}/v)$, where l is the length of the quartz container, v_{lim} is the critical velocity of quartz, and v is the neutron velocity. Since η is determined from the curve of storage after a fairly long delay time (when mainly only low-energy neutrons remain in the container), the correction $\Delta\eta$, for example, $v_{lim}/v \approx 2$ reaches 4×10^{-5}. Thus, the total loss coefficient is approximately 10^{-4}. In addition, the gap cannot in general be regarded as black. Neutrons that enter the gap can return to the container with a fairly large probability. This introduces an additional uncertainty into the interpretation of the experiments.

Finally, it is not clear from the results of the study what determines the excess loss coefficient. If it is due to the presence of hydrogen, there must be a temperature dependence of the loss coefficient. In particular, the storage curves in Fig. 6 must become straight in the initial section when the temperature is lowered but hardly change at long times, when the gaps play an important part. One of the temperature measurements was made in the study. When approximately half of the surface of the quartz container was heated to 40 °C, the storage curve changed qualitatively in agreement with the expectation. Moreover, it was possible to explain the change by assuming a dependence of the loss coefficient proportional to $\sqrt{T}$, i.e., by adopting the model of a free two-dimensional hydrogen gas on the surface.

In connection with attempts to find a temperature dependence of the loss coefficient, we should mention Refs. 65, 83, and 86. A temperature dependence was noted for the first time in the case of storage in an annealed aluminum container.[65] However, from the four points obtained in the study it was not possible to decide whether the excess loss coefficient is proportional to T or $\sqrt{T}$. In Ref. 83 (Fig. 7) it was found that in an annealed copper container with walls definitely contaminated by hydrogen the loss coefficient on lowering

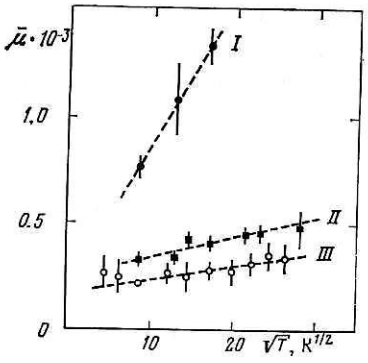

FIG. 7. Dependence of the loss coefficient μ on the temperature in an electrolytically polished copper container: I) without degassing; II) after degassing; III) the coefficient μ in a beryllium container.[83]

of the temperature changed rather appreciably, but after annealing there was hardly any temperature dependence. The same was observed in Ref. 86. In the figure, $\sqrt{T}$ is plotted along the abscissa, and thus the experiment appears to confirm the model of a two-dimensional gas, but the $\sqrt{T}$ hypothesis was not tested by likelihood criteria.

More definite indications of a $\sqrt{T}$ law were obtained in Ref. 87, in which it was shown that the excess loss coefficient is due largely to inelastic scattering, the inelastic-scattering cross section being proportional to $\sqrt{T}$. The experiment was made as follows. Piles of copper or beryllium plates were placed in a stream of ultracold neutrons. A thermal-neutron counter placed nearby detected neutrons heated on the plates. The reduced loss coefficient η of the plates was also measured. This was done by means of a storage chamber, in which the UCN storage time was measured with plates put into the chamber and without them. From the difference between the storage times in these two cases the coefficient η was determined. The plates were treated in different ways, each treatment leading to a corresponding coefficient η and flux of heated neutrons J_{tnd}. Constructing the dependence $\eta(J_{\text{tnd}})$, which must be linear, and extrapolating it to the point $J_{\text{tnd}} = 0$, we obtain the loss coefficient due solely to absorption. To within the errors, the extrapolated values of η agreed with the theory.

The temperature dependence of the cross sections was determined by measuring the average energy of the heated neutrons at different temperatures. This measurement was made by means of a chamber filled with ^{3}He and placed between the sample and the thermal-neutron detector. Determining the dependence of the count of the thermal-neutron detector on the pressure in the chamber, it was possible to find the average velocity of the heated neutrons. This velocity was found to be proportional to $\sqrt{T}$. And since the inelastic-scattering cross section is proportional to the average velocity, $\sigma_{\text{ie}} \sim \sqrt{T}$ as well. A further verification of this assertion is the measurement of the dependence $J_{\text{tnd}}(T)$. This dependence was found to have a shape close to $\sqrt{T}$. Thus, the experiment of Ref. 87 provided further support for the model of a two-dimensional hydrogen gas. However, a final conclusion would as yet be premature.

The results obtained in Ref. 145 contradict such a temperature dependence. In this experiment, ultracold neutrons were passed in a continuous stream through a chamber surrounded by thermal-neutron detectors (as in Fig. 4). The chamber was separated from the UCN detector and the neutron guide by aluminum windows, and an autonomous vacuum was maintained in the chamber. The chamber could be uniformly heated up to 800 °K or cooled to 80 °K. In addition, ^{4}He at different pressures could be admitted into it. The thermal-neutron detectors detected thermal neutrons formed in the chamber as the result of heating of the ultracold neutrons when they collided with the wall or with ^{4}He atoms. Overall, the complete system made it possible to determine separately the probability of heating and the probability of absorption of an ultracold neutron striking the wall. Moreover, it was possible to measure the temperature dependence of the probability of heating. This dependence was found to be linear to a good accuracy. In the measurements with degassed copper the relative fraction of inelastic scattering in the total loss coefficient agreed with the relative fraction of the cross section for inelastic scattering by the copper atoms in the total cross section, from which it follows that hydrogen contamination plays a small part. In the case of beryllium, however, the inelastic scattering strongly exceeded the theoretical scattering, and this may mean that hydrogen contamination of beryllium is fairly large.

A record storage time was obtained in the experiment of Ref. 146. In the experiment, D_2O vapor was frozen onto the walls of an aluminum container at 80 °K and very low-energy ultracold neutrons ($\sim$20 neV) were stored. Without the D_2O the storage time was 250 sec, but after the freezing of the D_2O it increased to 950 ± 60 sec, i.e., it was approximately equal to τ_β. However, this result contradicts the data of Ref. 81 and 47, in which D_2O freezing hardly influenced the storage time. It is possible that the technology used in the freezing has a decisive influence, and if the results of Ref. 146 are confirmed, then the aim—that of obtaining the maximal τ—can be regarded as achieved.

Magnetic Storage

Because of its magnetic moment, the neutron interacts with a magnetic field. The interaction energy $-\boldsymbol{\mu}\cdot\mathbf{B}$ is repulsive in nature when the neutron spin is parallel to the field $\mathbf{B}$, and attractive in the opposite case. If a region of space is surrounded by an inhomogeneous magnetic field, a neutron of sufficiently low energy will be repelled by the field when it is polarized parallel to it, and in this way one can achieve magnetic storage. As an example, we can give the magnetic field of a hexapole: $\mathbf{B} = cr^2\mathbf{e}$, where $r^2 = x^2 + y^2$, c is a constant, $\mathbf{e}$ is a unit vector in the (x, y) plane, $\mathbf{e} = (\sin 2\varphi, \cos 2\varphi)$, and φ is the azimuthal angle. A neutron can be stored in such a trap in a cylindrical region with the axis along z. If the hexapole is bent into a torus, a three-dimensional magnetic trap for ultracold neutrons is obtained.

Magnetic traps were first considered by Vladimirov,[7] who found the probability for spin flip of a neutron in passing near a region with zero field. If the neutron spin flips, the neutron ceases to be confined in the trap. To find how long a neutron will be stored in the trap, the equation

$$i\hbar\, d\xi/dt = -\hat{\mu}\mathbf{B}(t)\,\xi; \quad \hat{\mu} = \mu\sigma$$

for the spinor part of the neutron wave function (σ are the Pauli matrices) was solved in Ref. 88. To determine the dependence $\mathbf{B}(t)$, the neutron trajectory $\mathbf{r}(t)$ was specified, and it was assumed that $\mathbf{B}(t) = \mathbf{B}(\mathbf{r}(t))$. The probability of spin flip and, hence, loss of ultracold neutrons were found to be very small.

It is, however, interesting to examine this problem completely from the point of view of quantum mechanics. The point is that the neutron trajectory cannot be specified arbitrarily, since it is determined by the magnetic field. If it is assumed that the neutron always follows the field strictly, i.e., that its spin is parallel to the field, and the trajectory problem in the magnetic trap is solved classically, then in the hexapole field, in which the potential is proportional to r^2, we find that the radius vector of the true trajectory is equal to the square root of the radius vector of the elliptic trajectory. From the point of view of quantum mechanics, the potential is proportional to r^2 and characteristic of the harmonic oscillator, and therefore the problem for a neutron with spin parallel to $\mathbf{B}$ has a well-known solution. Can the neutron be strictly polarized along the field the whole time? The answer to this question is negative on the basis of the most general arguments. Indeed, the operator $p = \boldsymbol{\mu}\cdot\mathbf{B}/B = \boldsymbol{\mu}\cdot\mathbf{e}$ does not commute with the Hamiltonian, which contains the kinetic energy, and therefore it cannot have good, i.e., conserved quantum numbers. The Schrödinger equation[89]

$$[-(\hbar^2/2m)\,\Delta - \mu\mathbf{B}(\mathbf{r}) - E]\,\Psi(\mathbf{r}) = 0$$

for the neutron wave function is a system of two equations for the two components of the spin with cross terms, and these lead to spin flip with respect to $\mathbf{B}$. Without these terms, the behavior of ultracold neutrons in the field of, for example, a hexapole would be described by a system of discrete stable levels. Because of the cross terms, the labels are unstable, and it can be shown[89] that the higher a level, the more stable it is, whereas in ordinary quantum-mechanical problems the situation is quite the opposite. Only the lowest level is an exception. Here too it is absolutely stable. The probability of decay of a level is determined not only by its height but also by the form of the trajectory. The more elongated elliptical orbits decay faster than the circular ones.

The storage of neutrons in the magnetic field of a straight guide is very interesting. Here, neutrons in an attractive potential are stored, i.e., with spin opposite to the field, and if the total neutron energy is negative, the neutron spin cannot be flipped because of energy considerations. In this case, the cross terms have the consequence that the spin is not quite completely antiparallel to the field, and therefore the energy levels are slightly raised. The problem of the behavior of a neutron in the field of a direct current was solved in Refs. 90 and 91. In Ref. 91, an exact solution was obtained. Also interesting are traps of gravimagnetic type.[7,92] Here the neutrons are confined at the bottom by a magnetic field and at the top by the gravitational field.

Experiments with magnetic traps are described in Refs. 93–96. The traps took the form of a metallic cup, along the bottom and sides of which coils were placed, producing a magnetic field of alternating direction. In Refs. 94 and 95, a vacuum chamber of diameter 104 cm and height 34 cm was placed within the cup. The currents feeding the electromagnet reached 1000 A. It proved possible to accumulate about three neutrons in the trap. The magnetic storage time was 303 ± 37 sec.[95]

A similar experiment but with a smaller trap is described in Ref. 96. In this case it was possible to accumulate about one neutron per cycle, and the storage time was 35 ± 10 sec. As in Ref. 95, the reason for the comparatively short storage time in Ref. 96 was not known. In fact, work with the magnetic traps was begun because in a magnetic field there are no losses associated with absorption and heating by nuclei, and the storage time in the absence of depolarization should be equal to the intrinsic lifetime τ_β. Calculations of the depolarization for the simplest magnetic configurations of hexapole type show that in the majority of cases depolarization can be ignored. It is possible that some of the neutrons accumulated in the traps had an energy higher than the critical energy, and, since their number was small, the statistics was inadequate to permit more accurate measurement of the storage curve.

In this respect, the experiments with toroidal hexapole traps made at Grenoble[97] are of great interest. Figure 8 shows the storage curve of Ref. 98.

In a toroidal trap, one can keep neutrons of higher energies than the UCN energy, since for storage it is important that the neutrons be confined only in the direction perpendicular to the circular axis of the torus. In the given case, the average energy of the stored neutrons was about 2 μeV, which corresponds to a velocity of 20 m/sec. The higher the energy, the larger the number of neutrons that one can accumulate and the easier it is to measure the storage curve after a prolonged delay time. In the reduced storage curve one can see an initial section with a rapid decay, which can be attributed to neutrons from unstable orbits, and a long tail, whose slope determines the storage time of neutrons in stable orbits. The storage time of these neutrons was about 15 min, i.e., in agreement with the intrinsic neutron lifetime. A feature of the toroidal trap is that, first, it was made of a superconductor and had a maximal field of 3.5 T and, second, two poles facing into the torus were removed from it. These poles are unnecessary for storage, since the neutrons cannot approach the center of the torus on account of the centrifugal forces.

There is a further project for a magnetic trap of the type of a hexapole sphere (see, for example, the review of Ref. 99).

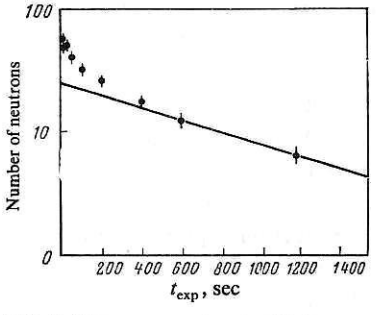

FIG. 8. Storage curve in a toroidal magnetic trap.[97,98]

It is a collection of three superconducting coils meridional with respect to the surface of the sphere. In such a trap an experiment to store sodium atoms was made. The storage time was about 1 sec. Because of numerous difficulties, this experiment was made only once and was not repeated. It is currently planned to use a spherical trap to store ultracold neutrons, which it is proposed to obtain directly within the trap by decelerating cold neutrons by means of liquid helium.

6. USES OF ULTRACOLD NEUTRONS

Many uses for ultracold neutrons have been pointed out recently. They can be divided into two types: fundamental, in which the investigated object is the neutron itself, and applied, in which the neutron is used as a tool to investigate matter. In the category of fundamental uses we have the search for an electric dipole moment, a gravitational moment, and a charge of the neutron, measurement of its intrinsic lifetime, the investigation of the wave properties of slow neutrons, interference and diffraction phenomena, and the search for possible neutron—antineutron oscillations. In the applied category, we have measurement of cross sections, investigation of the structure and dynamics of matter, and the problem of constructing a neutron microscope. Let us consider these problems in more detail.

Investigation of Fundamental Properties of the Neutron

Electric Dipole Moment. Let it be said right away that in speaking of a search for an electric dipole moment of the neutron one actually means interaction of the spin or the magnetic moment with an electric field: $\alpha \mathbf{s}\cdot\mathbf{E}$ or $\beta\boldsymbol{\mu}\cdot\mathbf{E}$ The constant α has the dimensions of the product of a charge and a length, $\alpha = eD$, i.e., the dimensions of an electric dipole moment. Such an interaction violates spatial and time symmetry, since if the direction of the spin s is identified with the angular-velocity vector of some rotation, it is reversed under time reversal and therefore the sign of the interaction with the electric field E changes and, in addition, even without time reversal the interaction $\mathbf{s}\cdot\mathbf{E}$ does not appear to have a right to exist, since the direction of s is a convention, i.e., it is chosen in accordance with the direction of motion of a right-handed screw and changes sign when a left-handed screw is chosen, whereas the energy of a physical interaction should not depend on convention. If the interaction $\mathbf{s}\cdot\mathbf{E}$ nevertheless exists, this means that right and left are no longer on an equal footing, i.e., there is no spatial symmetry. However, the present state of science shows that spatial and time parity are indeed violated, and therefore the search for an electric dipole moment of the neutron is fully justified. There are theoretical estimates of the dipole moment, which put it at $\sim 10^{-25}$ cm·e (see the review of Ref. 148).

An electric dipole moment can be measured in the same way as the magnetic moment of the neutron, i.e., by means of the resonance frequency of spin precession. In a magnetic field B, the spin precession frequency is $\omega = 2\mu B/\hbar$, but in the presence of an electric dipole moment and an external electric field $\mathbf{E}$ parallel or antiparallel to $\mathbf{B}$ the precession frequency is increased or decreased by $\alpha E/\hbar$, respectively. Thus, by measuring the change in the resonance frequency when the direction of the electric field is changed, one can find α or, if no changes are observed to within the limits of the statistical errors, establish an upper bound for the electric dipole moment.

Searches have been made for the moment using both neutrons with velocity 100 m/sec (Ref. 100) and ultracold neutrons.[101] As we noted earlier, the proposal to use ultracold neutrons to look for an electric dipole moment was made by Shapiro,[1] and the practical realization of the suggestion was carried out by the group of V. M. Lobashev at the Leningrad Institute of Nuclear Physics (Gatchina).[2]

To explain the idea of the experiment, let us suppose that ultracold neutrons are polarized along the field $\mathbf{B}$ and introduced into a trap in which there is not only the magnetic field $\mathbf{B}$ but also an electric field $\mathbf{E}$. During a short interval of time an rf resonance field $\mathbf{B}_1(t) \perp \mathbf{B}$ is applied, and this flips the neutron spin into the plane perpendicular to $\mathbf{B}$. After this, the rf field is switched away from the trap but the oscillator continues to work in order that there should be a memory of the phase of the rf field. When the rf field is switched away, the neutrons spin precesses around the fields $\mathbf{B}$ and $\mathbf{E}$ for a certain time T, after which the rf field is again applied to the trap and flips the spin in the direction opposite to the field $\mathbf{B}$. The neutrons are then released from the trap and their polarization is measured. If the frequency of the alternating field is exactly equal to the spin precession frequency and if $\alpha = 0$, then the second rf field will continue the action of the first as if the intermediate pause T had not existed, and the neutrons are completely polarized in the direction opposite to the field $\mathbf{B}$. If $\alpha \neq 0$, the precession frequency is slightly changed compared with the frequency of the alternating field, so that when the second rf field is applied the phases of the field and the spin are not matched, and the analyzer establishes a change in the polarization. For greater sensitivity of the experiment, the second rf field is additionally shifted in phase by $\pi/2$ and in the absence of an electric dipole moment is parallel to the spin if the spin precession frequency is equal to the frequency of the alternating field. As a result, the spin remains perpendicular to the field $\mathbf{B}$, i.e., the polarization of the neutrons along the field $\mathbf{B}$ is zero. In the presence of an electric dipole moment, there is a polarization proportional to α. When the direction of the field $\mathbf{E}$ is changed, the direction of the resulting polarization also changes.

We have just described the experiment in the so-called "storage variant."[102] In the "flow variant" two alternating fields are separated spatially. Figure 9 shows the arrangement of the experiment made at Gatchina.[101] In this experiment, the neutrons form a continuous stream, passing first the polarizer, the rf spin flipper, in which their spin is flipped into the plane perpendicular to $\mathbf{B}$, then through a chamber in which not only $\mathbf{B}$ but also an electric field $\mathbf{E}$ is applied, again through a spin flipper, through a polarization analyzer, and finally, a detector. There are two particular features of the experiment: first, the chamber is divided into two parts and the electric fields in them have opposite directions. This makes it possible to eliminate a spurious effect which arises when magnetic objects move relative to the apparatus. Second, to improve the statistics neutrons with both spin polari-

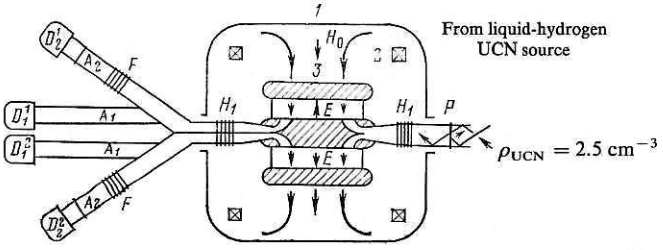

FIG. 9. Arrangement of experiment to measure the electric dipole moment of the neutron by means of ultracold neutrons: 1) magnetic screen; 2) coils; 3) UCN storage chambers; P is the polarizer, A_1 and A_2 are analyzers, D_1^1, D_1^2, D_2^1, D_2^2 are detectors; H_0 is a constant magnetic field, H_1 is an oscillating magnetic field, and E is an electric field.[101]

zations along the field **B** are detected, since they carry the same information, differing only in sign.[103]

In the experiment of Ref. 101, the neutrons diffuse from the polarizer to the analyzer. In the case of faster neutrons,[100] the experiment is done on a beam of particles flying rectilinearly. The faster neutrons have an advantage over the ultracold neutrons as regards intensity, but this is offset by the brevity of the time they remain in the region in which the field **E** is applied. In the case of the ultracold neutrons, $T \sim 10$ sec, whereas for the faster neutrons $T \approx 0.01$ sec. This means that using the ultracold neutrons one can achieve the same sensitivity as with faster neutrons even if the UCN flux is six orders of magnitude smaller. In fact, the difference between the intensities is less, and therefore UCN experiments are more sensitive. Ultracold neutrons have a further fundamental advantage. In a frame moving with a neutron, the electric field generates by virtue of relativistic effects the magnetic field $\Delta \mathbf{B} = \mathbf{v} \times \mathbf{E}/c$, where v is the neutron velocity. If **E** is not strictly parallel to **B**, which changes sign when **E** is switched and creates a parasitic effect difficult to take into account. This is a serious limitation on the sensitivity of experiments using thermal neutrons, in which a bound on the electric dipole moment has been obtained (3×10^{-24} cm·e, where e is the electron charge).[100] In the case of ultracold neutrons, the effect is much less, first, because of the lower velocity v and, second, the important thing is not the velocity itself but the velocity of diffusion of the neutron through the region with the field, which is appreciably less than v.

The most recent data obtained from the search for an electric dipole moment by means of ultracold neutrons correspond to the upper limit 4.3×10^{-25} cm·e.[2]

Important elements in these experiments are the polarizer[104] and the spin flipper.[105] Thermal neutrons are polarized largely by means of reflection from magnetized mirrors. Ultracold neutrons are conveniently polarized by passing them through a magnetized film. The critical energy of a magnetized material for the different spin components differs by $\pm \mu B$, where B is the internal field in the film. Neutrons with low critical energy pass through the film and are polarized in the direction opposite to the field B. It is be expected that the polarization must be 100%, since neutrons with the opposite spin cannot pass through the film. In practice, however, the polarization is about 85%. In the case of carefully prepared single crystal films[104] it can be raised to 98%.

Gravitational Dipole Moment.[106] As in the case of the electric dipole moment, one can consider the possible interaction of the spin with the gravitational field: $lmgs$, where g is the vector of the acceleration of free fall, and the constant l has the dimensions of length. This interaction also violates spatial and time symmetry and has the same right to exist as the electric dipole moment. It can also be sought by means of a resonance spin-precession experiment in gravitational and magnetic fields when they are parallel and antiparallel. However, in this case the gravitational field cannot be switched and the magnetic field must. To achieve the limit 10^{-24} cm·e in the measurement of the electric dipole moment, it is necessary to measure energy shifts of 10^{-19} eV. In the case of a gravitational dipole moment, such a shift corresponds to a constant $l = 10^{-10}$ cm, but it is necessary to control the magnetic field intensity when it is switched to accuracy 10^{-7} G. At the present time there is an experimental estimate of the gravitational dipole moment only for the proton[107]: $l < 10^{-5}$ cm.

Charge of the Neutron. There are in fact no grounds for believing that the neutron has a charge, but nor can such a possibility be ruled out. If the neutron should be found to carry a charge, this would have extremely important consequences in both elementary-particle phsyics and cosmology. Experiments looking for a charge are based on observing a small displacement of a neutron under the influence of an electric field. In an experiment with ultracold neutrons, it is hoped to lower the upper bound for the neutron charge to the level $(10^{-20}$–$10^{-21})e$.[108] There are reports[151] that by means of cold neutrons the limit has already been reduced to $q_n = (-1.5 \pm 2.2) \times 10^{-20} e$.

Neutron Lifetime. All the results hitherto obtained on the neutron lifetime τ_β were found in experiments involving β decay of the free neutron. In these experiments, the number of particles that are decay products is counted along a beam of thermal neutrons. The attained statistical error is 1%, but the results of different experiments[109–111,149] differ by 10%. This indicates that in the method there are systematic errors difficult to control.

By means of ultracold neutrons the experiment can be arranged differently with the neutron itself and not the decay products being observed. Such an approach is direct and may give a more reliable result. The essence of the experiment is to measure the storage time in a container: $1/\tau = 1/\tau_1 + 1/\tau_\beta$, finding the change in τ when τ_1 is changed. Since $1/\tau$ depends linearly on $1/\tau_1$, it is possible, by constructing the straight line $1/\tau(1/\tau_1)$, to extrapolate it to the point $1/\tau_1 = 0$, and the corresponding value of $1/\tau$ will be equal to $1/\tau_\beta$. In Ref. 112, a change in $1/\tau_1$ was achieved by changing the area S of the walls in the storage container, and $1/\tau_\beta$ was determined by extrapolating S to zero. The loss time is determined by the expression $\tau_1 = 4V/S\nu\mu$, where V is the volume of the container and μ is the loss coefficient. Therefore $1/\tau = 1/\tau_\beta + S\nu\mu/4V$. In the experiment of Ref. 112, the container was a vertical aluminum cylinder into which radial vertical baffles of the same aluminum were inserted. The

lifetime measured in this way was $\tau_\beta = 875 \pm 95$ sec. This accuracy is not the maximal possible. In future, it is hoped to reduce the error of measurement to 0.5%. To achieve this aim, it is necessary, in particular, to lower the value of η. By annealing the aluminum container in oxygen at 700 °K, it was possible to reduce η to 0.5×10^{-4}.[87] An even more promising result was obtained by freezing D_2O,[146] when $\eta\approx2\times10^{-5}$.

In principle, τ_1 can be changed differently.[113] If the loss coefficient is largely determined by inelastic scattering, then, changing the temperature of the walls, we simultaneously change τ_1. The change in τ_1 can be checked both by means of the total storage time τ and by observing neutrons heated at the walls. The latter makes it possible to determine $1/\tau_{ie}\approx1/\tau_1$. Extrapolating then to $1/\tau_1\to0$, we obtain $1/\tau_\beta$. Strictly speaking, this method leads after extrapolation to $1/\tau_\beta + 1/\tau_a$, where $\tau_a = \tau_1$ for $\sigma_{ie} = 0$. In the case of weakly absorbing materials such as graphite and beryllium, for which $\tau_\beta/\tau_a\approx0.01$, the extrapolated time is equal to τ_β to within 1%.

Neutron–Antineutron Oscillations. If as a result of some baryon-charge nonconserving interaction the neutron can go over to an antineutron, the probability of detecting an antineutron is higher, the longer the observation of the neutron is made. In this respect, ultracold neutrons are extremely convenient.[114] If the neutron and antineutron are reflected by the walls in approximately the same way, the probability of finding an antineutron in a container for ultracold neutrons is proportional to τ^2, where τ is the storage time. But if the reflection of the neutron and antineutron differ strongly, this probability is less: $\sim\tau t_f$, where t_f is the time between two collisions with the wall. Even in this case the probability of finding an antineutron is much greater than for thermal neutrons. Of course, ultracold neutrons are less intense, but even with allowance for this factor an experimental search for neutron–antineutron oscillations by means of ultracold neutrons may be more sensitive than an analogous experiment using faster neutrons.

Wave Properties of the Neutron

Diffraction. As a quantum-mechanical particle, the neutron is characterized by a de Broglie wavelength $\lambda = \hbar/mv$, which is longer, the lower the velocity v. For an ultracold neutron, $\lambda\sim100$ nm, i.e., it approaches the wavelength of ultraviolet light. It is interesting to consider how the diffraction and interference of neutrons with such long wavelengths occur. Diffraction by a diffraction grating with a specially chosen profile of the lines of the grating to concentrate the entire diffracted intensity in the first-order diffraction peak was observed in the experiment of Ref. 115. The grating had 1200 lines per 1 mm. The experimentally observed diffraction peak had width in good agreement with the resolution of the instrument. The absence of additional broadening indicates that the neutron coherence length covers not less than 100 lines, i.e., not less than 10^5 nm, which is an order of magnitude greater than the limit established earlier.[116]

Transmission of Films. Neutron interference phenomena have been studied in the transmission of thin matter films[117] and laminated systems.[118] Of particular interest is the transmission of a system of three layers, in which the central one has a lower potential than the two outer ones. The complete potential of the system has two humps. It has a high penetrability when an approximately integral number of wavelengths fits within the central part. This is equivalent to the presence of a resonance in the central layer. When neutrons pass through such a system, the intensity of the transmitted particles increases strongly at energies corresponding to the resonance. In the case of reflection from such a system, there is a dip in the intensity of the reflected neutrons at the resonance energy (see also Ref. 50). In a system of five layers,[118] which forms a three-hump potential, one resonance level is split into two. Figure 10 shows the transmission of such a system and the splitting of the resonance level into two separated by about 6 neV. This number shows what a high resolution can be achieved by means of ultracold neutrons.

Use of Ultracold Neutrons to Investigate Matter

Measurement of the Cross Sections of Homogeneous Substances. Total cross sections are measured by transmission. Since the cross sections for inelastic scattering and capture increase in proportion to $1/v$ with decreasing velocity, they play an important part in the transmission of ultracold neutrons. The aim of experiments with such neutrons is to test the $1/v$ dependence down to the lowest energies. It is interesting that near the critical energy (but, of course, above it) it is necessary in verifying the $1/v$ dependence to take into account the deceleration of the neutrons by the potential barrier and take as v the velocity within the material. These problems do not arise in the study of the transmission of gases, but it must here be borne in mind that the interaction of gas molecules with a neutron occurs effectively at the thermal velocities of the molecules, since the neutron can be regarded as being at rest compared with the molecules. Because of this feature, it is of interest to study the temperature dependence of the transmission of gases and, hence, the cross sections.

The transmission of solid homogeneous substances is usually described by the $1/v$ law.[120,121] The transmission of gases was studied in Refs. 122 and 123. It must be pointed out that in this case processes of gas adsorption on the surface of the container walls have a strong influence. Evidently, by studying gases one can simultaneously investigate

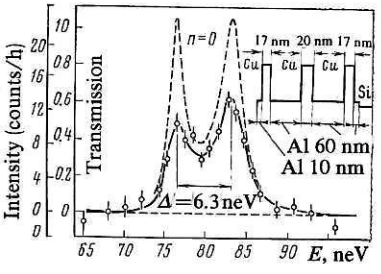

FIG. 10. Transmission of the five-layer system whose parameters are given in the insert. One can clearly see the splitting of the main resonance due to the coupling of two potential wells.[119]

their adsorption on the surfaces of different substances. It is also interesting to investigate whether clusters of gas molecules are formed.[80]

Investigation of the Structure of Matter. The transmission of many substances depends on the technology of their preparation and in many cases decreases with decreasing velocity faster than would follow for cross sections that grow in accordance with the law $1/v$. This can be explained by the presence in the substances of inhomogeneities with diameters of the order of tens or hundreds of nanometers, which lead to fairly strong elastic scattering. As an example, we can mention the measurement of the transmission of polycrystalline vanadium.[124] In an unannealed sample the total cross section increases when v is reduced below 35 m/sec in proportion to $v^{-2.8}$, but in the annealed sample the inhomogeneities disappear and the cross section varies as v^{-1}. As is shown in Ref. 125, by studying the energy dependence of the cross section at low energies it is possible to determine the parameters of the inhomogeneities within matter in the same way as is possible by means of small-angle scattering of thermal neutrons. As an example, an investigation was made[126] into the transmission of a suspension of amorphous SiO_2 spheres of diameter 13–14 nm. Fitting of the experimental transmission curve to the theoretical curve gave for the radius of the spheres 7.2 ± 2.1 nm, which indicates the effectiveness of the method. This method was used to study the ageing of AlZn alloys and the formation in them of Guinier–Preston zones enriched with zinc,[125] and also domains and domain walls in ferromagnets: nickel, iron, and cobalt.[127] Figure 11 shows how the dependence of the cross section on the neutron velocity changes in the case of transmission of a nickel sample (0.225-mm thick) in an external field as the field intensity is changed. At a high intensity of the external field the inhomogeneities disappear, the sample becomes uniformly magnetized, and the cross section depends on the velocity in accordance with the usual law $1/v$.

In Ref. 128, the method of small-angle scattering was compared with transmission of slow neutrons (note that, strictly speaking, these neutrons cannot be called ultracold, since for transmission their energy must be higher than the critical energy; such neutrons are generally said to be very cold). Of course, small-angle scattering gives richer information, but nevertheless the transmission of very cold neutrons may be preferable in some cases because of the simplicity of the experiment.

Neutron Microscope. The interaction of ultracold neutrons with matter can, as in the case of light, be described by a refractive index,[3,129] and therefore it is possible for such neutrons to have lenses and a microscope. However, the refractive index of materials depends on the energy E of the neutrons, $n = \sqrt{1 - \hbar^2 4\pi N_0 b / 2mE}$, and differs from unity appreciably only at energies 10^{-7} eV, at which the neutrons wavelength is about 100 nm.

The resolution of a neutron microscope is higher than that of a light microscope but much lower than that of an electron microscope. Why might one need a neutron microscope? The answer is rather simple. First, it can penetrate within opaque substances; second, it makes it possible to examine layers of matter too thick for an electron microscope; third, it is sensitive to the magnetic structure of matter, i.e., it makes it possible to obtain a magnetic image; and, finally, fourth, neutrons are sensitive to the chemical and isotopic composition of matter and therefore can detect structure where no structure can be seen in light rays because of the equal opacity with respect to light.[129] However, neutrons are sensitive to the gravitational field, and in the majority of optical systems this leads to strong chromatic aberration.[130] In principle, this aberration can be compensated in some way or other, for example, by compensating the gravitational field by a magnetic field if polarized neutrons are used or by choosing a definite geometry of the instrument and, finally, using compensating lenses made from different materials. In three experiments a neutron image has been obtained by means of ultracold neutrons. In the first,[131] a vertical concave mirror was used to obtain an image of three vertical slits. In the second,[132] the image of a horizontal slit was magnified by six times. The optical element in this case was a concave mirror proposed earlier[133] with a Fresnel zone plate deposited on it. In such a system, the chromatic aberration is compensated. In the third study,[134] a radiographic, i.e., shadow, image of strips of different materials placed in front of a scintillation sector equipped with photographic film was obtained. It is possible that in the future such work on forming images by means of ultracold neutrons will be more widespread.

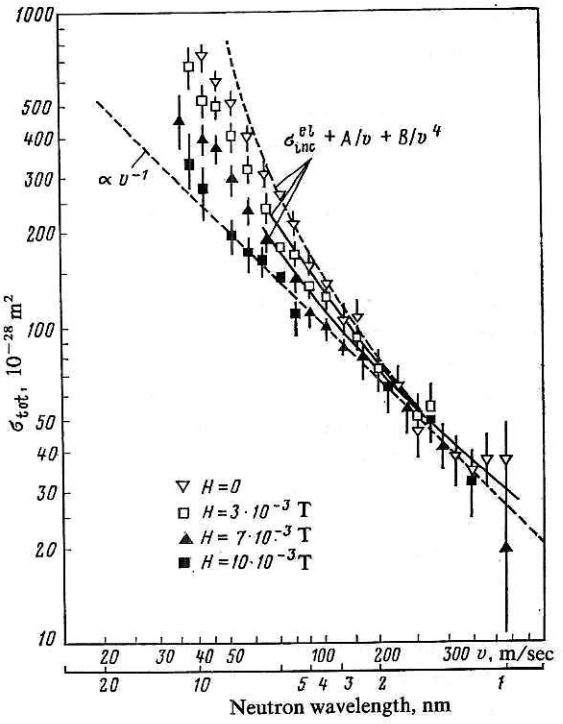

FIG. 11. Dependence on the neutron velocity v of the total cross section of nickel for different intensities of the external magnetic field. The broken curve corresponds to the $1/v$ behavior of the cross section; the continuous curves are obtained by fitting to the experimental points. The parameter A characterizes the cross section of absorption and inelastic scattering, while B characterizes the scattering of domains and domain walls.[127]

CONCLUSIONS

Up to now, the number of studies on ultracold neutrons exceeds 350. It is clear that even the mere mention of each study would require much more space than there is in the present paper. Therefore, we have not here been able to give an exhaustive review and we apologize to authors whose works we have not considered. For a better acquaintance with the problems of ultracold neutrons, we can recommend the reviews of Refs. 14 and 135–142. Investigations with ultracold neutrons are now being made in many countries: England, Bulgaria, the Soviet Union, the United States, Canada, France, the German Federal Republic, and Japan. This is explained by the attractive features and comparative simplicity of the investigated object. Some investigators are interested in the ultracold neutrons themselves and the problem of storing them; others, in the possible applications. There is no doubt that the possibilities of using ultracold neutrons and the tasks they can perform will increase with the passage of time. In particular, advance into the region of even lower energies is beginning.[143] Spectrometers with high resolution will be constructed and inelastic scattering experiments with small energy transfer will be performed, and this will be helpful, for example, for biology. New possibilities are opened up for investigation in the field of surface physics and surface structures (for example, measurement of the parameters of elements of roughness), dynamics, and adsorption. There is no doubt that experiments with ultracold neutrons will also make a contribution to technology. Neutorn microscopy will be developed, etc.

Of course, this does not exhaust all the possible directions, some of which may become clear only in the future. But it is to be hoped that what we have discussed here is sufficient to give the reader a true picture of the promise of investigations in the field of ultracold neutrons.

[1]F. L. Shapiro Usp. Fiz. Nauk **95**, 145 (1968) [Sov. Phys. Usp. **11**, 345 (1969)].
[2]I. S. Altarev *et al.*, Inst. Phys. Conf. Ser. No. 62, 633 (1982).
[3]I. M. Frank, in: Intern. Conf. on Nuclear Structure Study with Neutrons (Budapest, 1972) (eds. J. Ero and J. Szucs), Plenum Press, New York (1972), p. 285.
[4]I. M. Frank, Materialy II Mezhdunarodnoĭ shkoly po neĭtronnoĭ fizike (Proc. of the Second Intern. School on Neutron Physics), D3-7991, JINR, Dubna (1974), p. 19.
[5]Ya. B. Zel'dovich, Zh. Eksp. Teor. Fiz. **36**, 1952 (1958) [Sov. Phys. JETP **9**, 1389 (1959)].
[6]G. M. Drabkin and R. A. Zhitnikov, Zh. Eksp. Teor. Fiz. **38**, 1013 (1960) [Sov. Phys. JETP **11**, 729 (1960)].
[7]V. V. Vladimirskiĭ, Zh. Eksp. Teor. Fiz. **39**, 1062 (1960) [Sov. Phys. JETP **12**, 740 (1961)].
[8]I. I. Gurevich and P. É. Nemirovskiĭ, Zh. Eksp. Teor. Fiz. **41**, 1175 (1961) [Sov. Phys. JETP **14**, 838 (1962)].
[9]I. I. Gurevich and L. V. Tarasov, Fizika neĭtronov nizkikh énergiĭ (Physics of Low Energy Neutrons), Nauka, Moscow (1965), p. 287.
[10]L. L. Foldy, in: Preludes in Theoretical Physics (eds. A. de Shalit, H. Feshbach, and L. van Hove), North-Holland, Amsterdam (1966), p. 205.
[11]V. I. Lushikov, Yu. N. Pokotilovskiĭ, A. V. Strelkov, and F. L. Shapiro, Pis'ma Zh. Eksp. Teor. Fiz. **9**, 40 (1969) [JETP Lett. **9**, 23 (1969)].
[12]A. Steyerl, Phys. Lett. **29**, 33 (1969).
[13]I. M. Frank, Soobshchenie (Communication) R3-9846, JINR, Dubna (1976).
[14]V. V. Golikov, V. I. Lushchikov, and F. L. Shapiro, Zh. Eksp. Teor. Fiz. **64**, 73 (1973) [Sov. Phys. JETP **37**, 41 (1973)].
[15]E. Z. Akhmetov, D. K. Kaipov, V. A. Konks, *et al.*, in: Neĭtronnaya fizika (Neutron Physics), Vol. 2, TsNIIatominform, Moscow (1976), p. 155.
[16]F. L. Shapiro, Fiz. Elem. Chastits At. Yadra **2**, 973 (1972) [Sov. J. Part. Nucl. **2**, Part 4, 96 (1972)].
[17]Yu. Yu. Kosvintsev *et al.*, Nucl. Instrum. Methods **143**, 33 (1977).
[18]I. S. Altarev, Yu. V. Borisov, A. V. Brandin, *et al.*, Phys. Lett. **A80**, 413 (1980).
[19]R. Golub and J. M. Pendlebury, Phys. Lett. **A62**, 337 (1977).
[20]P. Ageron *et al.*, Phys. Lett. **A66**, 469 (1978).
[21]A. V. Antonov, D. E. Vul', and M. V. Kazarnovskiĭ, Pis'ma Zh. Eksp. Teor. Fiz. **9**, 307 (1969) [JETP Lett. **9**, 180 (1969)].
[22]A. Steyerl, Nucl. Instrum. Methods. **125**, 461 (1975).
[23]N. T. Kashukeev, Nucl. Instrum. Methods **125**, 43 (1975).
[24]I. O. Brun, J. M. Carpenter, V. E. Krohn, *et al.*, Phys. Lett. **A75**, 223 (1980).
[25]F. Mezei, Commun. Phys. **1**, 81 (1976).
[26]M. Utsuro, S. Shirahama, K. Okamura, *et al.*, in: Proc. of the Fourth Intern. Collaboration on Advanced Neutron Sources (ICANS-IV) KEK, Isukuba, October 20–24, KENS Rep. II. Lab. for High Energy Physics (eds. Ishikawa *et al.*) (1981), p. 743.
[27]L. V. Groshev, V. N. Dvoretsky, A. M. Demidov, *et al.*, Phys. Lett. **B34**, 293 (1971).
[28]F. L. Shapiro, in: Intern. Conf. on Nuclear Structure Study with Neutrons (Budapest, 1972) (eds. J. Ero and J. Szucs), Plenum Press, New York, p. 259.
[29]A. Steyerl, Z. Phys. **254**, 169 (1972).
[30]I. Berceann and V. K. Ignatovich, Vacuum **23**, 441 (1973).
[31]M. Brown *et al.*, Vacuum **25**, 61 (1975).
[32]Yu. Yu. Kosvintsev, Yu. A. Kushnir, V. I. Morozov, and A. P. Platonov, in: Neĭtronnaya fizika (Neutron Physics), Vol. 2, TsNIIatominform, Moscow (1976), p. 193.
[33]A. I. Egorov, V. M. Lobashov, V. A. Nazarenko, *et al.*, Yad. Fiz. **19**, 300 (1974) [Sov. J. Nucl. Phys. **19**, 147 (1974)].
[34]N. T. Kashukeev and N. F. Chikov, Soobshchenie (Communication) R3-82-45, JINR, Dubna (1982).
[35]E. Z. Akhmetov *et al.*, in: Neĭtronnaya fizika (Neutron Physics), Vol. 2, TsNIIatominform, Moscow (1976), p. 150.
[36]W. Mysenholder, Nucl. Instrum. Methods **137**, 291 (1976).
[37]V. K. Ignatovich and G. I. Terehov, Nucl. Instrum. Methods **148**, 585 (1978).
[38]A. V. Antonov, O. F. Galkin, A. E. Gureĭ, *et al.*, Pis'ma Zh. Eksp. Teor. Fiz. **24**, 387 (1976) [JETP Lett. **24**, 352 (1976)].
[39]M. I. Novopltsev and Yu. N. Pokotilovsky, Nucl. Instrum. Methods **171**, 497 (1980).
[40]M. V. Kaipov, A. D. Stoĭka, A. V. Strelkov, and M. Hetzelt, Soobshchenie (Communication) R3-12271, JINR, Dubna (1979).
[41]L. V. Groshev, V. N. Dvoretskiĭ, A. M. Demidov, *et al.*, Soobshchenie (Communication) R3-7282, JINR, Dubna (1973); in: Neĭtronnaya fizika (Neutron Physics), Vol. 4, TsNIIatominform, Obninsk (1974), p. 264.
[42]W. Mampe *et al.*, Z. Phys. **45**, 1 (1981).
[43]A. V. Antonov *et al.*, Kratk. Soobshch. Fiz. **10**, 11 (1974).
[44]A. V. Antonov, Preprint No. 86 [in Russian], P. N. Lebedev Physics Institute, Moscow (1973).
[45]V. N. Dvoretskiĭ, Preprint No. 2715 [in Russian], Institute of Atomic Energy, Moscow (1976).
[46]Yu. Yu. Kosvintsev, Yu. A. Kushnir, and V. I. Morozov, in: Neĭtronnaya fizika (Neutron Physics), Vol. 1, TsNIIatominform, Moscow (1977), p. 156.
[47]Yu. Yu. Kosvintsev, Yu. A. Kushnir, and V. I. Morozov, in: Neĭtronnaya fizika (Neutron Physics), Vol. 1, TsNIIatominform, Moscow (1980), p. 116.
[48]V. K. Ignatovich and G. I. Terekhov, Soobshchenie (Communication) R4-9567, JINR, Dubna (1976).
[49]A. Steyerl, Nucl. Instrum. Methods **101**, 295 (1972).
[50]M. I. Novopol'tsev and Yu. N. Pokotilovskiĭ, Preprint R3-81-828 [in Russian], JINR, Dubna (1981).
[51]L. L. Foldy, Phys. Rev. **67**, 107 (1945).
[52]V. K. Ignatovich and V. I. Lushchikov, Soobshchenie (Communication) R3-8795, JINR, Dubna (1975).
[53]A. Grossmann, R. Høegh-Krohn, and M. Mebkhout, Commun. Math. Phys. **77**, 87 (1980).
[54]V. K. Ignatovich, Soobshchenie (Communication) R4-10778, JINR, Dubna (1977).
[55]V. K. Ignatovich, Soobshchenie (Communication) E4-11937, JINR, Dubna (1978).
[56]V. K. Ignatovich, Soobshchenie (Communication) R4-6681, JINR,

Dubna (1972).
[57]V.K. Ignatovich, Phys. Status Solidi B **71**, 477 (1975).
[58]Rutherford and Appleton Laboratories, Particle Physics Experiments, RL-81-001 (1980), p. 37.
[59]V. E. Zhitarev, A. M. Motorin, and S. B. Stepanov, At. Energ. **50**, 350 (1981).
[60]V. I. Lushchikov, S. A. Nikolaev, Yu. N. Panin, *et al.*, Preprint No. 3066 [in Russian], Institute of Atomic Energy, Moscow (1978).
[61]Yu. Yu. Kosvintsev, Yu. A. Kushnir, and V. I. Morozov, in: Neĭtronnaya fizika (Neutron Physics), Vol. 2, TsNIIatominform, Moscow (1976).
[62]I. M. Frank, Soobshchenie (Communication) R4-8851, JINR, Dubna (1975).
[63]A. S. Gerasimov, V. K. Ignatovich, and M. V. Kazarnovskiĭ, Kratk, Soobshch. Fiz. No. 8, 56 (1973); Preprint R4-6940 [in Russian], JINR, Dubna (1973).
[64]L. V. Groshev, V. I. Lushchikov, S. A. Nikolaev, *et al.*, in: Neĭtronnaya fizika (Neutron Physics), Vol. 2, TsNIIatominform, Moscow (1975), p. 166.
[65]Yu. Yu. Kosvintsev, Yu. A. Kushnir, and V. I. Morozov, Zh. Eksp. Teor. Fiz. **77**, 1277 (1979) [Sov. Phys. JETP 642 (1979)].
[66]V. M. Galitskiĭ and L. M Satarov, Preprint No. 2657 [in Russian], Institute of Atomic Energy, Moscow (1976).
[67]V.K. Ignatovich, Soobshchenie (Communication) R4-7055, JINR, Dubna (1973).
[68]A. V. Stepanov and A. V. Shelagin, Kratk. Soobshch. Fiz. No. 1, 12 (1974).
[69]Yu. M. Kagan, Pis'ma Zh. Eksp. Teor. Fiz. **11**, 235 (1970) [JETP Lett. **11**, 147 (1970)].
[70]V. K. Ignatovich, Soobshchenie (Communication) R4-7831, JINR, Dubna (1974).
[71]I. M. Frank, Soobshchenie (Communication) R3-7809, JINR, Dubna (1974).
[72]V. K. Ignatovich, Soobshchenie (Communication) E4-8039, JINR, Dubna (1974).
[73]V. K. Ignatovich and V. I. Lushchikov, Soobshchenie (Communication) R4-81-77, JINR, Dubna (1981).
[74]A. D. Stoika, A. V. Strelkov, and M. Hetzelt, Z. Phys. **29**, 349 (1978).
[75]W. A. Landford and R. Golub, Phys. Rev. Lett. **39**, 1509 (1977).
[76]V. K. Ignatovich and L. M. Satarov, Preprint No. 2820 [in Russian], Institute of Atomic Energy, Moscow (1977).
[77]D. I. Blohintsev and N. M. Plakida, Phys. Status Solidi B **82**, 627 (1977).
[78]V. K. Ignatovich, in: Materialy shkoly LIYaF po fizike kondensirovannykh sred (Proc. of the School of the Leningrad Institute of Nuclear Physics on the Physics of Condensed Media), Leningrad (1979), p. 216.
[79]N. M. Plakida, Soobshchenie (Communication) R17-81-91, JINR, Dubna (1981).
[80]V. K. Ignatovich, Soobshchenie (Communication) R4-80-261, JINR, Dubna (1980).
[81]Yu. Yu. Kosvintsev, Yu. A. Kushnir, V. I. Morozov, *et al.*, Pis'ma Zh. Eksp. Teor. Fiz. **28**, 164 (1978) [JETP Lett. **28**, 153 (1978)].
[82]J. P. Bugeat and W. Mampe, Z. Phys. **B35**, 273 (1979).
[83]Yu. Yu. Kosvintsev, Yu. A. Kushnir, V. I. Morozov, *et al.*, Soobshchenie (Communication) R3-80-91, JINR, Dubna (1980).
[84]P. H. La Marche *et al.*, Nucl. Instrum. Methods **189**, 533 (1981).
[85]W. Mampe *et al.*, Z. Phys. **B45**, 1 (1981).
[86]I. M. Frank, Soobshchenie (Communication) R3-12829, JINR, Dubna (1979), p. 16.
[87]V. I. Morozov, Khranenie UKhN v zamknutykh sosudakh (Storage of Ultracold Neutrons in Closed Containers), NIIAR, Dimitrovgrad (1982).
[88]I. M. Matora, Yad. Fiz. **16**, 624 (1972) [Sov. J. Nucl. Phys. **16**, 349 (1973)].
[89]V. K. Ignatovich, Soobshchenie (Communication) E4-8404, JINR, Dubna (1974).
[90]V. K. Ignatovich and Yu. N. Pokotilovskiĭ, Soobshchenie (Communication) R4-101145, JINR, Dubna (1976).
[91]G. P. Pron'ko and Yu. G. Stroganov, Pis'ma Zh. Eksp. Teor. Fiz. **24**, 196 (1976) [JETP Lett. **24**, 171 (1976)].
[92]V. K. Ignatovich and G. I. Terekhov, Soobshchenie (Communication) R4-10102, JINR, Dubna (1976).
[93]Yu. G. Abov, V. F. Belkin, V. V. Vasil'ev, *et al.*, Preprint No. 44 [in Russian], Institute of Theoretical and Experimental Physics, Moscow (1976).
[94]Yu. G. Abov, V. F. Belkin, S. P. Borovlev, *et al.*, Preprint No. 16 [in Russian], Institute of Theoretical and Experimental Physics, Moscow (1981).
[95]Yu. G. Abov *et al.*, Preprint No. 21 [in Russian], Institute of Theoretical and Experimental Physics, Moscow (1982).
[96]Yu. Yu. Kosvintsev, Yu. A. Kushnir, V. I. Morozov, and I. A. Plotnikov, Pis'ma Zh. Eksp. Teor. Fiz. **27**, 70 (1978) [JETP Lett. **27**, 65 (1978)].
[97]K. J. Kugler, W. Paul, and U. Irinks, Phys. Lett. **B72**, 422 (1978).
[98]CERN Courier **17**, 365 (1977).
[99]R. Golub, W. Mampe, J. M. Pendlebury, and P. Ageron, Sci. Am. **240**, No. 6, 106 (1979).
[100]N. F. Ramsey, Phys. Rep. **63**, 410 (1978).
[101]I. S. Altarev, Yu. A. Borisov, N. Y. Borovikova, *et al.*, Phys. Lett. **B102**, 13 (1981).
[102]Yu. V. Taran, Soobshchenie (Communication) R3-7149, JINR, Dubna (1973).
[103]Yu. V. Taran, Soobshchenie (Communication) R3-8442, JINR, Dubna (1974); in: Neĭtronnaya fizika (Neutron Physics), Vol. 1, TsNIIatominform, Moscow (1977), p. 200.
[104]R. Herdin, A. Steyerl, A. R. Taylor, *et al.*, Nucl. Instrum. Methods **148**, 353 (1978).
[105]Yu. V. Taran, in: Neĭtronnaya fizika (Neutron Physics), Part. 6, TsNIIatominform, Moscow (1976), p. 211.
[106]R. Golub, in: Fundamental Physics Research with Reactor Neutrons and Neutrinos, IPCS 42 (1978), p. 104.
[107]B. V. Vasil'ev, Pis'ma Zh. Eksp. Teor. Fiz. **9**, 299 (1969) (JETP Lett. **9**, 175 (1969)].
[108]N. T. Kashukeev and N. F. Chikov, Bolg. Fiz. Zh. **6**, 529 (1979).
[109]A. N. Sosnovsky *et al.*, Nucl. Phys. **10**, 395 (1959).
[110]C. J. Christensen *et al.*, Phys. Rev. **50**, 1628 (1972).
[111]L. N. Bondarenko *et al.*, Pis'ma Zh. Eksp. Teor. Fiz. **28**, 328 (1978) [JETP Lett. **28**, 303 (1978)].
[112]Yu. Yu. Kosvintsev, Yu. A. Kushnir, and V. I. Morozov, Pis'ma Zh. Eksp. Teor. Fiz. **31**, 257 (1980) [JETP Lett. **31**, 236 (1980)].
[113]A. V. Antonov *et al.*, Kratk. Soobshch. Fiz. No. 1, 41 (1982).
[114]K. G. Chetirkin *et al.*, Phys. Lett. **B99**, 358 (1981).
[115]H. Scheckenhofer and A. Steyerl, Phys. Rev. Lett. **39**, 1310 (1977).
[116]C. G. Shull, Phys. Rev. **179**, 752 (1969).
[117]A. Steyerl, Z. Phys. **252**, 351 (1972).
[118]K. A. Steinhauser, A. Steyerl, H. Scheckenhofer, and S. D. Malik, Phys. Rev. Lett. **44**, 1306 (1980).
[119]A. Steyerl, T. Ebisowa, K. A. Steinhauser, and M. Utsuro, Z. Phys. **B41**, 283 (1981).
[120]A. Steyerl and H. Vonach, Z. Phys. **250**, 166 (1972).
[121]A. V. Antonov, A. I. Isakov, I. V. Meshkov, *et al.*, Kratk. Soobshch. Fiz. No. 11, 13 (1978).
[122]Yu. Yu. Kosvintsev, Yu. A. Kushnir, V. I. Morozov, and G. I. Terekhov, in: Neĭtronnaya fizika (Neutron Physics), Part 1, TsNIIatominform, Moscow (1980), p. 130.
[123]E. Z. Akhmetov *et al.*, Izv. Akad. Nauk Kaz. SSR No. 6, 14 (1981).
[124]A. V. Antonov, I. V. Isakov, A. D. Meshkov, *et al.*, Kratk. Soobshch. Fiz. No. 9, 43 (1978).
[125]A. Steyerl, D3-7991, JINR, Dubna (1974).
[126]M. Lengsfeld and A. Steyerl, Z. Phys. **B27**, 117 (1977).
[127]A. Steyerl and R. Lerner, Phys. Status Solidi A **33**, 531 (1976).
[128]G. Engelmann, A. Steyerl, A. Heidemann, *et al.*, Z. Phys. **B35**, 345 (1979).
[129]I. M. Frank, Priroda **9**, 24 (1972).
[130]A. I. Frank, in: Neĭtronnaya fizika (Neutron Physics), Part 1, TsNIIatominform, Moscow (1980), p. 150.
[131]N. T. Kashukeev and N. F. Chikov, Pis'ma Zh. Eksp. Teor. Fiz. **30**, 306 (1979) [JETP Lett. **30**, 283 (1979)].
[132]G. Schutz, A. Steyerl, and W. Mampe, Phys. Rev. Lett. **44**, 1400 (1980).
[133]A. Steyerl and G. Schütz, Appl. Phys. **17**, 45 (1978).
[134]J. C. Bates, Phys. Lett. **A83**, 29 (1981).
[135]F. L. Shapiro, Soobshchenie (Communication) R3-7135, JINR, Dubna (1973).
[136]V. I. Luschikov, Phys. Today **30**, 42 (1977).
[137]V. I. Morozov, At. Energ. **45**, 442 (1978).
[138]V. I. Morozov, NIIAR. Obzornaya informatsiya (Review Information), Dimitrovgrad (1980).
[139]A. I. Frank, Priroda, No. 1, 30 (1981).
[140]A. Steyerl, Springer Tracts Mod. Phys. **80**, 57 (1977).
[141]R. Golub and J. M. Pendlebury, Rep. Prog. Phys. **42**, 439 (1979).
[142]K. F. Smith, Contemp. Phys. **21**, 631 (1980).
[143]V. I. Lushchikov and A. I. Frank, Pis'ma Zh. Eksp. Teor. Fiz. **28**, 607 (1978) [JETP Lett. **28**, 559 (1978)].
[144]V. F. Turchin, Medlennye neĭtrony (Slow Neutrons), Gosatomizdat, Moscow (1963), p. 25.

[145]V.K. Ignatovich, V. I. Lushchikov, *et al.*, Soobshchenie (Communication) R3-82-822, JINR, Dubna (1982).
[146]Yu. Yu. Kosvintsev, V. I. Morozov, and G. I. Terekhov, Pis'ma Zh. Eksp. Teor. Fiz. **36**, 346 (1982) [JETP Lett. **36**, 424 (1982)].
[147]A. A. Akunets *et al.*, Kratk. Soobshch. Fiz. No. 1, 25 (1982).
[148]A. P. Serebrov, in: Materialy XVI Zimneĭ shkoly LIYaF (Proc. of the 14th Winter School of the Leningrad Institute of Nuclear Physics), Leningrad (1979), p. 3.
[149]J. Byrn *et al.*, Phys. Lett. **B72**, 422 (1980).
[150]N. M. Kadykenov *et al.*, Preprint 12–82 [in Russian], Institute of Nuclear Physics, Alma-Ata (1982).
[151]R. Gahler *et al.*, Phys. Rev. D **25**, 2887 (1982).
[152]R. Golub *et al.*, Z. Phys. **51**, 187 (1983).

Translated by Julian B. Barbour